# Effect of petrographic characteristics on physico-mechanical properties of Granitic gneisses from Islampur and Shir Atraf areas, Swat, NW Pakistan.


**ILYAS MEHMOOD MUHSIN**

**M.Phil. Geology**

**Department of Earth Sciences**

**Faculty of Natural Sciences**

**Quaid-i-Azam University**

**Islamabad, Pakistan**

**2022**

# Effect of petrographic characteristics on physico-mechanical properties of Granitic gneisses from Islampur and Shir Atraf areas, Swat, NW Pakistan.

A Thesis Submitted to Quaid-i-Azam Islamabad in the partial fulfilment of requirements for the Degree of **"Master of Philosophy in Geology"**


By

**Ilyas Mehmood Muhsin**

**Supervised by**

**Dr. Abbas Ali Naseem**

**Department of Earth Sciences**

**Quaid-i-Azam University Islamabad**

**Pakistan**


**2022**

## Dedication

*This work is dedicated to my respected teachers and loving family members. Especially to my grandmother, who is a wellspring of prayers for me.*

# ABSTRACT

To determine the effect of petrographic characteristic on physico-mechanical properties of Swat granitic gneisses field studies combined with petrographic and physico-mechanical investigations were conducted. The field observations indicate that the studied rocks are granitic gneisses. Based on the field and petrographic characteristics the exposed granitic rocks in both areas i.e., Shir Atraf and Islampur granitic gneisses were divided into different varieties. The Shir Atraf granitic gneisses were divided to two different varieties such as Shir Atraf medium grained variety and Shir Atraf coarse grained variety. The Islampur granitic gneisses were divided in to three different varieties Islampur fine grained variety, Islampur medium grained variety and Islampur coarse grained variety.

Petrographic study reveals that the essential minerals found in all varieties are quartz, alkali feldspar and plagioclase. Biotite, muscovite, epidote, chlorite, garnet, tourmaline, and ore minerals are also present in minor to accessory amount. To determine the physico-mechanical properties Uniaxial Compressive Strength (UCS), Uniaxial Tensile Strength (UTS), specific gravity, water absorption, and porosity were performed. Different graphs have drawn to show the possible relationship between petrographic characteristics and physico-mechanical properties.

In conclusion, based on above studies (i.e., petrographic studies and physico-mechanical properties) reveal that the mineralogical composition, grain shape, grain size, density, grain-size distribution, micro-fractures, grain contact types, degree of weathering, cleavage planes, all have an impact on mechanical properties. According to IAEG (International Association of Engineering Geologists) standards, the analysed rocks' UCS values are strong, whereas ISRM (International Society of Rock Mechanics) standards place them in the moderate to high strength category. The UCS and UTS values, as well as porosity, water absorption, and specific gravity, are all within acceptable limits for usage as construction material in heavy projects such as highways, buildings, tunnels, dams, and railway tracks.

# ACKNOWLEDGEMENT

First, thanks to Allah almighty the most gracious the most merciful. All my respect is for the most praiseworthy prophet Muhammad (S.A.W) who is the cause of conceiving this universe and by his conduct showed us the right path.

I am profoundly thankful to my supervisor **Dr. Abbas Ali Naseem,** Assistant Professor, Department of Earth Sciences, Quaid-i-Azam University Islamabad for his guidance and support. Without his guidance and persistent help this thesis would not have been possible. No word has yet been invented through which I can express my respect, gratitude, and feelings for my supervisor.

My days in the university would not have been much more memorable had had I not met quality friends, namely, Mr. Kashif Anwar, Mr. Said Mukhtar Ahmad, Mr. Naveed Iqbal, Mr. Sikandar Shah, Dr. Akbar Ali and Mr. Kaleem Ullah. The time spent and all the good and bad memories with these friends will always be a reason to smile in my life.

It the end I am indebted to my family members for their trust, support and all the prayers.

**ILYAS MEHMOOD MUHSIN**

# LIST OF CONTENTS

Dedication……..……..i

Abstract ……..……..……ii

Acknowledgement …….……...…...…….iii

Lists of contents……..…..…….iv

List of Figures ……...….viii

List of Tables ……...……...…….xii

**CHAPTER 1**

**INTRODUCTION** ……1

1.1.General Statement ……... 1

1.2. Study Area Location, Topography, and Climate ……... 2

1.3. Previous Work ……2

1.4. Scope ……..3

1.5. Aims and Objectives ……...3

1.6. Methodology ……...4

**CHAPTER 2**

**REGIONAL GEOLOGY** ……...……..……...6

2.1. General Statement ……...6

2.2. Karakoram Block ……6

2.3. Kohistan Island Arc ……7

2.4. Indian Plate Himalayan Sequence ……..7

2.4.1. Tethyan Himalayan Sequence ……8

2.4.2. Higher Himalayan Sequence ……...8

2.4.3. Lesser Himalayan Sequence ……...8

2.4.4. Sub Himalayan Sequence ……...8

2.5. Local Stratigraphy ……..……9

2.5.1. Manglaur Formation ……..…..9

2.5.2. Swat Granitic Gneisses ……..……9

2.5.3. Alpurai Group ……...10

a. Marghazar Formation ……...10

b. Kashala Formation ……..10

c. Saidu Formation ……10

d. Nikanai Ghar Formation ……..11

**CHAPTER 3**

**METHADOLOGY** ……..12

3.1. General Statement ……12

3.2. Review of Literature ……..12

3.3. Field Investigation ……12

3.4. Sample Collection ……12

3.5. Sample Coding ……13

3.6. Core Sample Preparation for Mechanical Tests ……13

3.7. Laboratory Work ……..14

3.7.1. Geotechnical Laboratory Work ……..…14

3.7.2. Petrographic Laboratory Work ……14

a. Thin Sections Preparation ……14

b. Thin Sections Studies ……14

3.8. Structure of Thesis ……15

**CHAPTER 4**

**PETROGRAPHY** ……16

4.1. General Statement ……16

4.2. Field Investigation ……16

4.3. Petrography ……...19

4.3.1. Shir Atraf Granitic Gneisses ……19

a. Coarse Grained Variety ……19

b. Medium Grained Variety ……24

4.3.2. Islampur Granitic Gneisses ……29

a. Coarse Grained Variety ……29

b. Medium Grained Variety ……..32

c. Fine Grained Variety ……... 37

**CHAPTER 5**

**PHYSICAL AND MECHANICAL PROPERTIES** ……42

5.1. General Statement ……42

5.2. Physical and Mechanical Properties ……43

5.2.1. Strength Tests ……43

a. Uniaxial Compressive Strength ……...44

b. Uniaxial Tensile Strength ……45

5.2.2. Specific Gravity ……47

5.2.3. Porosity ……..47

5.2.4. Water Absorption ……..47

**CHAPTER 6**

**RELATIONSHIP AMONG PETROGRAPHIC, PHYSICAL AND MECHANICAL PROPERTIES**…….52

6.1. General Statement …….52

6.2. UCS VS Q/F Ratio ……53

6.3. UCS VS Quartz ……54

6.4. UCS VS Porosity ……...55

6.5. UTS VS Q/F Ratio ……56

6.6. UCS VS Water Absorption ……57

6.7. UCS VS Mica ……58

6.8. UCS VS UTS ……59

6.9. Q/F Ratio VS Porosity …… ……60

6.10. Quartz VS Porosity ……61

**CHAPTER 7**

**DISCUSSION AND CONCLUSION** ……62

7.1. General Statement ……62

7.2. Petrography ……...62

7.3. Mechanical Properties ……...63

7.4. Conclusion ……65

**REFRENCES** ……67

# List of Figures

**Fig 1.1.** Generalized geological map showing the major alkaline complexes in Northern Pakistan (after Pogue et al., 1999; Khattak et al., 2005) marked box showing location of the study area. ……..5

**Fig. 2.1.** Comparative structural/stratigraphy columns from lower swat, modified from DiPietro (1990). ……...11

**Fig. 4.1.** (A) Shir Atraf granitic gneisses (B) Coarse grained variety (C) Medium grained variety ……17

**Fig. 4.2.** Islampur granitic gneisses (A) Coarse grained variety (B) Medium grained variety

(C) Fine grained variety ……...18

**Fig. 4.3.** Photomicrographs: (A, PPL; B, XPL) (B) Orthoclase, the red arrow showing undulose extinction in quartz and green arrow showing muscovite grain. ……21

**Fig. 4.4.** Photomicrographs: (A, PPL; B, XPL) (B) Microcline, orthoclase, plagioclase, quartz, biotite, the red arrows showing muscovite grains and green arrow showing myrmekitic texture in orthoclase grain. ……...22

**Fig. 4.5**. Photomicrographs: (A, PPL; B, XPL) (B) Quartz, orthoclase, muscovite, the red arrow showing Carlsbad-albite twinning in plagioclase and green arrow showing oscillatory zoning in plagioclase grain. ……22

**Fig. 4.6**. Photomicrographs: (A, PPL; B, XPL) (A) the white arrows showing biotite grains, (B) Microcline, the red arrows showing quartz inclusion and yellow arrow showing muscovite grain inclusion in microcline. ……...23

**Fig. 4.7.** Photomicrographs: (A, PPL; B, XPL) (A) tourmaline grains, (B) Plagioclase, orthoclase, the red arrows showing tourmaline grains, green arrows showing muscovite grains, blue arrow showing ore mineral and the white arrows showing biotite grains. ……23

**Fig. 4.8.** Photomicrographs: (A, PPL; B, XPL) (A) Garnet, tourmaline, biotite grains, (B) Orthoclase, quartz, garnet, tourmaline, the blue arrows showing quartz inclusion, green arrows showing muscovite grains and red arrows showing microcline. ……...24

**Fig. 4.9.** Photomicrographs: (A, PPL; B, XPL) (B) Quartz, orthoclase, muscovite, the red arrow showing tourmaline, green arrow showing patchy extinction in quartz grain and blue arrow showing biotite grain. ……...26

**Fig. 4.10.** Photomicrographs: (A, PPL; B, XPL) (B) Quartz, biotite, the red arrows showing epidote and blue arrows showing chlorite. ……...27

**Fig. 4.11.** Photomicrographs: (A, PPL; B, XPL) (B) Muscovite, the red arrows showing oscillatory zoning in plagioclase grain. ……...27

**Fig. 4.12.** Photomicrographs: (A, PPL; B, XPL) (B) Orthoclase, plagioclase, microcline, muscovite, biotite, the red arrow showing patchy extinction in quartz grain. ……...28

**Fig. 4.13.** Photomicrographs: (A, PPL; B, XPL) (A) Garnet, biotite (B) Orthoclase, plagioclase, muscovite, the red arrow showing poikilitic texture in orthoclase grain. ……..28

**Fig. 4.14.** Photomicrographs: (A, PPL; B, XPL) (A) the red arrows showing the ores grains, the yellow arrow showing biotite (B) green arrows showing muscovite grains. ……..29

**Fig. 4.15.** Photomicrographs: (A, PPL; B, XPL) (A) the green arrows showing biotite grains (B) Orthoclase, muscovite, biotite, the red arrows showing biotite ultration to epidote and chlorite. ……31

**Fig. 4.16.** Photomicrographs: (A, PPL; B, XPL) (B) Microcline, the red arrow showing undulose extinction in quartz (inclusion of biotite also present). ……31

**Fig. 4.17.** Photomicrographs: (A, PPL; B, XPL) (A) white arrow showing ore grain, red arrows showing biotite grains (B) many microcline grains, muscovite. ……...32

**Fig. 4.18.** Photomicrographs: (A, PPL; B, XPL) (B) Orthoclase, quartz, plagioclase, muscovite. ……32

**Fig. 4.19.** Photomicrographs: (A, PPL; B, XPL) (A) Biotite, the red arrows showing garnet grains (B) Orthoclase, quartz, plagioclase, muscovite. ……34

**Fig. 4.20.** Photomicrographs: (A, PPL; B, XPL) (A) brown tourmaline (B) plagioclase, muscovite, the red arrows showing Carlsbad-albite twinning in plagioclase. ……...35

**Fig. 4.21.** Photomicrographs: (A, PPL; B, XPL) (B) Plagioclase, orthoclase, muscovite, the red arrow showing undulose extinction in quartz. ……..35

**Fig. 4.22**. Photomicrographs: (A, PPL; B, XPL) (B) orthoclase (perthitic texture), plagioclase, the green arrow showing biotite ultration to epidote and chlorite, the blue arrow showing muscovite. ……36

**Fig. 4.23.** Photomicrographs: (A, PPL; B, XPL) (A) The red arrows showing biotite grains (B) Microcline, orthoclase (perthitic texture) and quartz. ……..36

**Fig. 4.24**. Photomicrographs: (A, PPL; B, XPL) (A) Biotite (some grains in needle form), some fine ore grains (B) Quartz (polycrystalline), orthoclase, plagioclase, microcline. ……38

**Fig. 4.25**. Photomicrographs: (A, PPL; B, XPL) (A) the red arrow showing ore grain, the green arrows showing biotite grains. (B) orthoclase (quartz inclusion are present), the white arrow showing Myrmekitic texture in orthoclase grain, the blue arrow showing perthitic texture in orthoclase grain. ……..39

**Fig. 4.26**. Photomicrographs: (A, PPL; B, XPL) (B) Quartz (polycrystalline), orthoclase (quartz inclusion are present), plagioclase, microcline, the red arrows showing muscovite grains. ……..39

**Fig. 4.27.** Modal composition of the studied rocks plotted on the IUGS classification diagram (from Le Maitre, 2002). ……41

**Fig. 5.1**. Universal testing machine (UTM), sample for UCS test and Universal testing machine (UTM), sample for UTS test…….. ……...50

**Fig. 5.2**. Rock cutting machine ……51

**Fig. 6.1.** Relationship between UCS and Q/F ratio: (A) Shir Atraf granitic gneisses (B) Islampur granitic gneisses. ……...53

**Fig. 6.2.** Relationship between UCS and Quartz: (A) Shir Atraf granitic gneisses (B) Islampur granitic gneisses. ……..54

**Fig. 6.3**. Relationship between UCS and porosity: (A) Shir Atraf granitic gneisses (B) Islampur granitic gneisses. ……..55

**Fig. 6.4**. Relationship between UTS and Q/F ratio: (A) Shir Atraf granitic gneisses (B) Islampur granitic gneisses. ……..56

**Fig. 6.5**. Relationship between UCS and water absorption: (A) Shir Atraf granitic gneisses (B) Islampur granitic gneisses. ……...57

**Fig. 6.6**. Relationship between UCS and Mica content: (A) Shir Atraf granitic gneisses (B) Islampur granitic gneisses. ……...58

**Fig. 6.7**. Relationship between UCS and UTS: (A) Shir Atraf granitic gneisses (B) Islampur granitic gneisses. ……..59

**Fig. 6.8**. Relationship between porosity and Q/F ratio: (A) Shir Atraf granitic gneisses (B) Islampur granitic gneisses. ……...60

**Fig. 6.9**. Relationship between Quartz and porosity: (A) Shir Atraf granitic gneisses (B) Islampur granitic gneisses. ……...61

# List of Tables

**Table 4.1.** Modal composition of Shir Atraf and Islampur granitic gneisses ……...40

**Table. 5.1**. Showing UTS values ……45

**Table. 5.2.** Showing UTS values. ……46

**Table. 5.3.** Showing specific gravity, porosity, and water absorption values. ……..48

**Table. 5.4.** Showing all combine value of UCS, UTS, specific gravity, porosity, and water absorption values. ……49

**Table 7.1.** Grades of unconfined compressive strength ……...64

**Table 7.2.** Average values of UCS, UTS, porosity, water absorption, specific gravity, quartz to feldspar ratio and mica content of the studied samples. ……64

# CHAPTER 1 INTRODUCTION

## 1.1. General Statement

Granitic rocks are abundant in the continental crust and form abundant basement rocks that are overlain by relatively thin continental strata. Granitic rocks can be found in many places in NW Pakistan, either as large batholiths or as small intrusions (Tahirkheli and Jan., 1979). Based on tectonic, geochemical, petrographic, radiometric, and geographical data the granitic rock of north Pakistan was categorised into five categories by Jan et al., (1981). Granitic gneisses of Nanga Parbat, Mansehra, and Swat areas, alkaline granites of Tarbila, Shewa Shahbazgarhi, Ambila, Malakand and Warsak.

The lower Swat region is located south of the MMT and is the north portion of the Indo-Pak plate. The lower Swat comprises mostly of metamorphic rock that is classified as basement and sequence rock, whereas the Manglaur Formation includes basement rock and Swat granitic gneisses, and the meta sedimentary layer is made up of the lithologies that comprise the Alpurai group (DiPietro., 1990).

In Pakistan, there are some notable examples of Pb-Zn-Mo and Ur (uranium) mineralization associated with granitic rocks of the NW Himalayas (Butt, 1983). Some of these granitic rocks and associated pegmatites contain gemstones such as topaz, tourmaline, aquamarine, sphene, zircon, and others (Jan and Kazmi., 2005).

Granites are commonly used as dimensional stones and as construction materials in the design of bridge foundations, dams, buildings, towers, highways, railways, spillways, canals, and so on. It's also used to design underground excavations like tunnels, mines, and other underground chambers. The uses of granitic rocks are totally dependent on mechanical properties and the petrographic characteristics such as grain shape, fabric, mineral composition, modal mineralogy, recrystallization, grain contacts, degree of deformation, degree of interlocking fractures and weathering all have a significant impact on mechanical properties (Irfan., 1996).

## 1.2. Study Area location, topography, and climate

In the present study two different areas were mentioned where Swat grinitic gneisses were exposed. These areas are Islampur and Shir Atraf villages, Swat KPK, Northern Pakistan. The granitic gnisses are easily accessible beside the main road of Islampur and Shir Atraf village. The geographical location of the sampling area in Islampur is 34.717 deg latitude 72.371 deg longitude, and the geographical location of the sampling area in Shir Atraf 34.695 deg latitude 72.359 deg longitude. The average elevation above sea level is 1190 meter.

In climate summer season in Saidu Sharif are long, hot, and clear, with an average daily high temperature of 85 degrees Fahrenheit from May to September. With a temperature of 98 degrees Fahrenheit, June 21 is the warmest day of the year. The winter season are cold and partly cloudy, for 3 to 4 months from December to March. With a temperature of 34 degrees Fahrenheit, January 9 is the coldest day of the year. The month of August saw the most rainfall, with an average total accumulation of 2.7 inches.

## 1.3. Previous work

Martin et al., (1962) were the first to whose worked on the stratigraphy of the lower Swat region. The kings., (1964). Arif et al., (2002) investigated the petrographic features of the Swat granitic gneisses and determined that the Swat gneisses include a tiny amount of tourmaline, a quartz-feldspathic vein system that is generally medium grained, and almost equi-granular.

Similarly, (DiPietro., Pogue et al., 1993) investigated the stratigraphy, metamorphism and structures of the lower Swat areas and identified their structural framework and depositional sequence. The Swat granitic gneisses were classified into two kinds by DiPietro., (1990). The flaser granitic gneisses have a light colour and coarse grain, whereas the Augen gneisses have a dark colour and fine grain. Based on similarities with Mansehra granitic gneisses, Shams., (1969) proposed a Cambrian to Ordovician age for Swat granitic gneisses. The Rb-Sr isotope was used to establish the emplacement date of the Swat granitic gneisses (Khan., Ahmad et al., 2019). Lawangin Sheikh et al., (2020) worked on geochronology and geochemistry of the Swat orthogneisses. Previous work on Swat granitic gneisses was conducted by many authors, but information on the physico-mechanical properties of these rocks is mainly absent. Many authors have worked to find a relation between petrographic characters and the mechanical behavior of rocks (Shakoor and Bonelli, 1991; Howarth and Rowlands, 1987; Akessan et al., 2003; Sajid et al., 2009). In the current geological research, samples of granitic gneisses from

the Islampur and Shir Atraf areas of Swat district were examined both petrographically and geotechnically to determine the nature and absence of any probable relationship between their petrographic characters and geo-mechanical properties.

## 1.4. Scope

Granites are commonly used as dimensional stones and as construction materials in the design of bridge foundations, dams, buildings, towers, highways, railways, spillways, canals, and so on. It's also used to design underground excavations like tunnels, mines, and other underground chambers. The uses of rocks are totally dependent on mechanical properties and the petrographic characteristics such as grain shape, fabric, mineral composition, modal mineralogy, recrystallization, grain contacts, degree of deformation, degree of interlocking fractures and weathering all have a significant impact on mechanical properties (Irfan., 1996).

## 1.5. Aims and objectives

The goal of this research is to investigate the precise petrography and physico-mechanical characteristics of Swat granitic gnisses to develop relevant petrographic and physico-mechanical relationships and to evaluate the suitability of these rocks for construction applications.

The following are the objectives of the current research:

1. Petrographic study of Swat granitic gneisses for determining its modal mineralogical composition.
2. Understanding the physico-mechanical properties of Swat granitic gneisses through various tests (UCS, UTS, porosity, specific gravity, water absorption), and determining their suitability for use as construction material and dimension stone in accordance with international standards.
3. To establish a relation between the selected rock's physico-mechanical properties and petrographic characteristics of these rocks.
4. In terms of physico-mechanical and petrographic features, distinct textural types of the Swat granitic gneisses were compared to one other.

## 1.6. Methodology

For detailed petrographic study and physico-mechanical analysis, five bulk samples were collected from several textural types in Islampur and Shir Atraf areas, Swat. The geographic locations of bulk samples collection area were recorded. Several significant field features were photographed and noted. At Hanan Tech Pakistan, Mansehra, cores from each type were taken from a bulk sample using a core cutting machine and strength tests of rock cores were performed at NCEG Geotechnical lab University of Peshawar. From each of these samples thin sections were prepared for petrographic study in the Rock Cutting laboratory of Bacha Khan University, Charsadda. In the Petrographic laboratory of Department of Earth Sciences, Quaid I Azam Islamabad, each thin section has studied.

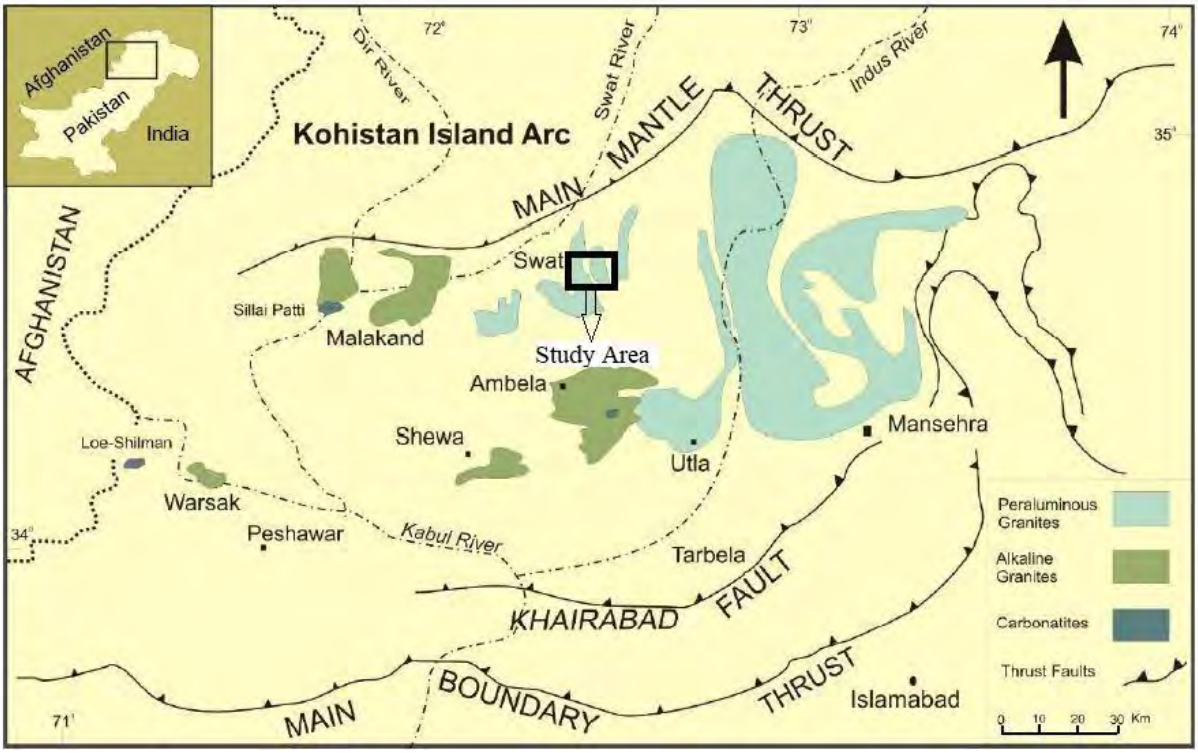


Fig 1.1. Generalized geological map showing the major alkaline complexes in Northern Pakistan (after Pogue et al., 1999; Khattak et al., 2005) marked box showing location of the study area.

# CHAPTER 2 REGIONAL GEOLOGY AND STRATIGRAPHY

## 2.1. General Statement

The north Pakistan areas are located on the north part of the Indian plate and the Eurasian plate, with rocks ranging from Precambrian to Tertiary in age. Corward et al., (1984) classified north Pakistan into three tectonic domains: the Karakoram block (Eurasian plate), the Kohistan Island Arc, and the Indian plate sequence.

The Karakoram block is the southernmost portion of the Eurasian plate. From north to south, Gaetani et al., (1996) and Searle et al., (1999) classified the Karakoram terrane into three units. The first one is northern sedimentary belt, the central one is Karakoram batholith, and the last one is southern metamorphic unit.

The Kohistan Island arc (KIA) is a sandwich-like structure formed by the Eurasian plate and the Indian plate within the Tethys Ocean. Toward the north of KIA is bounded MKT with Eurasian plate (Karakoram block) and MMT is present toward the south of KIA with Indian plate. In the Eocene age, the KIA collided with the Karakoram microplate between 70 and 100 million years ago, and the KIA was abducted on the Indian plate Searle et al., (1999).

The Indian plate separated from the Gondwana landmass around 130 Ma and drifted 5000 kilometres in the Paleogene toward the Eurasian plate's margin and closing the Tethys Ocean (Klootwijk et al., 1992; Petterson and Treloar, 2004; Molnar and Tapponnier., 1975). In the Eocene, the Eurasian and Indian plates collide. As a result of this collision, the northern margin of the Indo-Pak is made up of crystalline thrust sheets from the Himalayan orogenic belt.

## 2.2. Karakoram Block

The karakoram block is about 70 to 120-km-wide and 1400-km-long block (Kazmi and Jan., 1997). This block is separated from Pamir block by Pamir fault (Desio and Martina, 1972), and separated to the east by the Karakoram fault (Kazmi and Jan., 1997). Main Karakoram Thrust or Karakoram-Kohistan suture zone or Shyok Suture Zone marked boundary between the Karakoram micro plate and KIA. (Gansser, 1980; Thakur, 1981; Tahirkheli, 1982; Thukur and Misra., 1984). Karakoram block was classified into three units by Debon et al., 1987; and Gaetani et al., 1996. Northern sedimentary belt, Karakoram batholiths, and southern Karakoram metamorphic unit.

## 2.3. Kohistan island arc

Between the Eurasian plate and Indian plate, the sandwich like structure and form within the Tethys is Kohistan Island arc. According to Searle et al., (1999), KIA collided with Karakoram microplate between 70 and 100 Ma, and KIA was abducted on the Indian plate in the Eocene. MKT marked the boundary between KIA and Karakoram block and MMT marked the boundary between KIA and Indian plate. MMT is the western extension of the Indus Tsango suture zone (Treloar et al., 1989).

The khan et al., (1997) divided the KIA into five units extending from ISZ to SSZ.

- Jijal complex
- Kamila amphibolite
- Chilas complex
- Kohistan batholith
- Chalt volcanics

The Jijal, Sapat, and Torra Tigga complexes are essentially basic ultramafic cumulates bodies that occur along the KIA's southern edge (Ahmed and Chaudhry, 1976; Jan et al.,1983; Jan and Tahirkheli, 1990; Jan and Windley, 1990). Kamila Amphibolite can be found in the southern portion of the arc (Jan.,1977 and 1980). The Chilas complex is a mafic to ultramafic intrusive body that runs 300 kilometres east to west in a 40-kilometer-wide arc (Khan etal.,1989). This complex is a massive mafic intrusion that contains gabbro-norite as well as lesser ultramafic intrusive bodies such as pyroxenites, dunnite, harzburgites, troctolites, anorthosites, and hornblende gabbro (Khan et al., 1989, 1993). Along the northern margin of KIA Chalt Volcanic Group rocks are present (Petterson and Windley., 1991; Petterson and Treloar., 2004).

## 2.4. Indian Plate Himalayan Sequence

The Indian plate contained the crystalline thrust sheets of Himalayan orogenic belt. ITSZ marked a boundary between KIA and Indian plate (Dipetro et al., 2000). The Himalayan Mountain Range spreads over 2500 kilometres from the Brahmaputra to the Indus River, with a thickness of 200-250 kilometres (Le Forte., 1975). From north to south, the Himalayan sequence of the Indian plate is separated into four tectono-stratigraphic zones by the base of its major bounding faults (Gansser., 1964; Gansser., 1981; LeFort, 1975 and Hodges., 2000).

- Tethyan Himalaya
- Higher Himalaya
- Lesser Himalaya
- Sub-Himalaya

### 2.4.1 Tethyan Himalayan Sequence

The Tethyan Himalayan sequence is found on the Indian plate's northern passive margin and contain carbonate and siliciclastic sedimentary rock (Baud, 1984, Garzanti et al., 1987; Gaetani and Garganit., 1991). On the north, the Tethyan Himalayas are terminated by the Indus-Tsango suture zone.

### 2.4.2 Higher Himalayan Sequence

The higher Himalayan sequence, which lies between the MCT and the STD (South Tibetan detachment system), frequently contains high grade metamorphic rock (DiPietro et al., 2004). The Higher Himalaya sequence Is the Indian Plate's most northernly exposed region, consisting of a thick succession of high-grade metamorphic rocks. It is composed mainly of Lower Proterozoic augen orthogneiss and Upper Proterozoic to Cambrian augen orthogneiss. Another notable aspect of the Higher Himalayan Crystalline zone is the presence of tourmaline-bearing leucogranites (Hodges., 2000; Pognante et al., 1990; Gansser., 1964).

### 2.4.3. Lesser Himalaya Sequence

The MCT (Main Central Thrust) runs through the Lesser Himalaya series to the north, and the MBT (Main Boundary Thrust) runs toward the south. The Lesser Himalaya sequence is the foothill of the Himalayan sequence, and it contains a variety of lithologies such as quartzite, shale, orthogneisses, psammitic phyllites, and impure marble (Colchen et al., 1988; Valdiya, 1980 and Gansser., 1964).

### 2.4.4. Sub Himalaya Sequence

The outer Himalayan zone, also known as Siwalik or outer Himalayan zone. It made up of an 8,000- to 10,000-meter-thick pile of sedimentary rock (Burbank et al., 1997). From Punjab to Assam, the sub-Himalayan range consists of Siwalik and Murree molasse. The southern sequence of folded Siwalik is covered by alluvium, which is interrupted by the Himalayan frontal fault in the foothill's region. The boundary between the sub and lesser Himalaya is MBT (M Rustam Khan et al., 2016). MFT (Main Frontal Thrust) split the sub-Himalayan sequence from the alluvium plains. (Lave and Avouac, 2000; Yeats and Lillie, 1991).

## 2.5. local Stratigraphy

The lower Swat is situated in the Himalayan foothills (DiPietro et al., 1993). Martin et al., (1962) and King (1964) defined a sequence of quartz-schist, amphibolite, calc-schist, and phyllite as the lower Swat schistose group, with tourmaline and Augen granitic gneisses intruding at the base.

According to DiPietro (1990), the strata exposed to the south of MMT in the Indian plate includes the Precambrian-Cambrian (?) Mangluar Formation, an unknown-age Jobra Formation, and late Paleozoic to early Mesozoic Alpurai group rock. Manglaur Formation comprises of garnetiferous schist, tremolite and quartzite marble and the Manglaur Formation is intruded by Swat of augen-flaser granitic gneisses. An erosional unconformity separates these units from the Alpurai group (DiPietro., 1990).

There are four Formations in the Alpurai group. At the base, the amphibolitic Marghazar Formation is overlain by calc-schists and marbles from the Kashala Formation. Saidu Formation's graphitic phyllites are at the top of the sequence in north, but the Saidu is replaced by marbles from the Nikanai Ghar Formation in the south. The earliest Formation is the Marghazar, which is overlain by the Kashala Formation, followed by the Nikanai Ghar Formation, and finally the Saidu Formation (Pogue et al., 1993).

### 2.5.1. Mangluar Formation

The Mangluar Formation is the oldest unit of lower Swat, intruded by Swat granitic gneisses and unconformably overlain by Alpurai group rocks (DiPietro., 1990). Mangluar Formation gets its name from Mangluar village, which is located 10 kilometres east of Saidu (Kazmi et al., 1984). This Formation includes schists (garnetiferous schists, graphitic schist, biotite schist), tremolite marble, and amphibolite (DiPietro, Pogue et al., 1993).

### 2.5.2. Swat Granitic Gneisses

Swat granitic gneisses intrude the Manglaur Formation. The grade of metamorphism of Swat granitic gneisses is not well clarified, but Shams (1969) suggests that they are strongly related to Mansehra gneisses and that the grade of metamorphism should be high. Based on similarities with Mansehra granitic gneisses, Shams (1969) assumed a Cambrian to Ordovician age for Swat granitic gneisses.

DiPietro (1990) divided these granitic gneisses into two, the flaser granitic gneisses (light-colored, coarse-grained ground mass) and the Augen granodiorite gneisses (dark-colored, fine-

grained ground mass). The Augen granodiorite gneisses and the flaser granitic gneisses are both contemporaneous, however the latter intrusive phase occurs later. The flaser granitic gneisses and the Augen granodiorite gneisses have a gradational contact at Loesar. In several areas, another sharp and concordant contact exists between the Swat granitic gneisses and the Mangluar Formation.

### 2.5.3. Alpurai Group

The Alpurai group is on top of the Manglaur Formation and Swat gneisses (Kazmi et al., 1984). Pogue et al., (1992) classified the Alpurai group into four Formations: Marghazar, Kashala, Saidu, and Nikanai Ghar. The Alpurai group rocks are Precambrian in age (Chaudhry et al., 1992).

#### a. Marghazar Formation

The name Salampur Formation was described by Chaudhry et al., (1992), but the name Marghazar Formation was described by DiPietro et al., (1999) because the type locality is located along the stream of Marghazar village. Schist (garnetiferous muscovite schist, epidote-biotite schist, amphibolitic schist and rare graphitic schist also present), marble, and amphibolite dominate the Marghazar Formation (DiPietro et al., 1993).

#### b. Kashala Formation

From the MMT to the Peshawar Basin, the Kashala Formation underlies a large area of lower Swat. Kashala got its name from the Kashala Mountain Dop Sar, which is located about 13 kilometres southwest of Saidu Sharif (DiPietro et al., 1993). The main lithologies in the Dop Sar area are garnet and epidote-bearing calcareous schist, which grades into schistose marble and then into coarsely crystalline brown or grey calcite marble. The Kashala Formation has a lower sharp contact with the Marghazar Formation's amphibolitic layer (DiPietro et al., 1993).

#### c. Saidu Formation

The Saidu Formation is a continuous belt that runs parallel to the MMT and overlies the Kashala Formation (DiPietro et al., 1993). Martin et al., (1962) give the name phyllitic schists, Saidu schist by Kazmi et al., (1962) and graphic schists by Ahmed et al., (1987). The type of location is a long road cut (east of Mingora) approximately one kilometre to the north of Saidu Sharif (Martin et al., 1962, Kazmi et al., 1984). This Formation is primarily composed of graphitic, phyllite and marbles.

### d. Nikanai Ghar Formation

Nikanai Ghar Formation is a massive lens-shaped body located in the south-central part of Lower Swat (DiPietro., 1990). The name is derived from Nikanai Ghar, which is located approximately 25 kilometres south of Saidu. According to DiPietro et al., (1999), the Nikanai Ghar Formation is composed of white to grey thick or massively bedded, fine to coarse grain marble, and dolomitic marble. There are also thin beds of calcareous schist, graphitic phyllite, calcareous quartzite, and schistose marble.

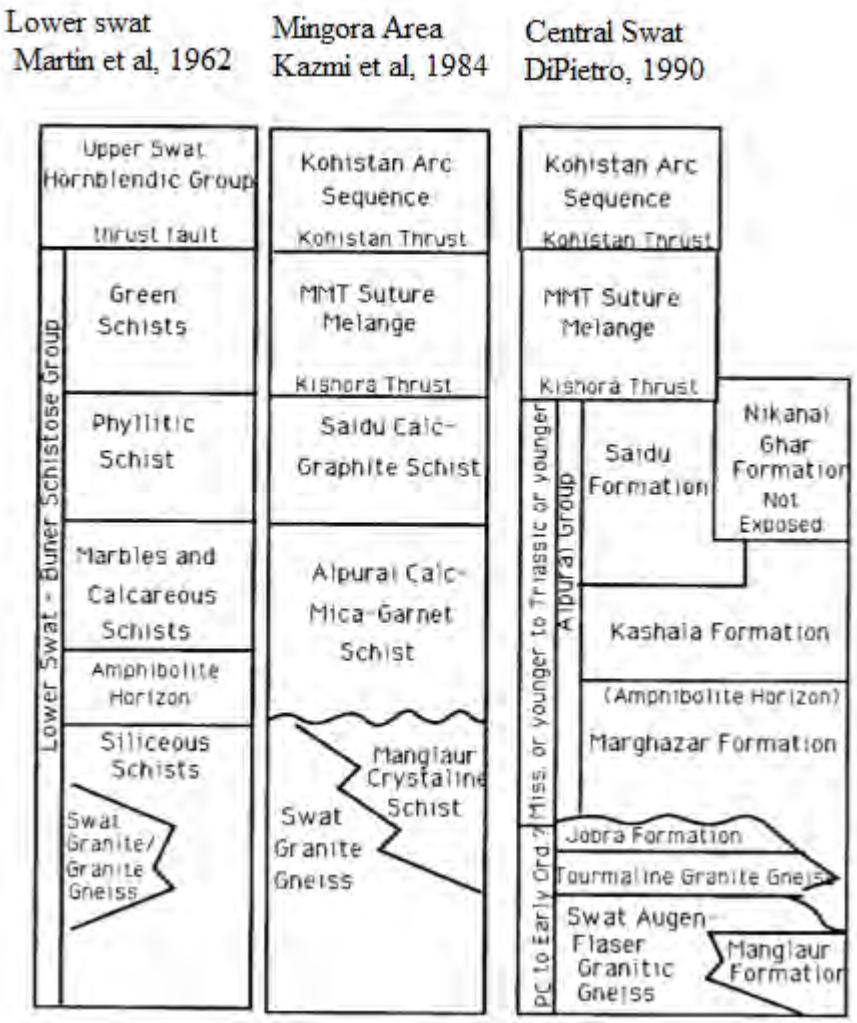


Fig. 2.1. Comparative structural/stratigraphy columns from lower Swat, modified from DiPietro (1990).

# CHAPTER 3 RESEARH METHODOLOGY

## 3.1. General statement

Before the field investigation and laboratory work, we need detail literature review. After the literature review the field investigation and laboratory work were performed. In field investigation the various geological features identification is so important for example foliation, lineation, strata identification, weathered and fresh surface identification etc. There were no apparent fractures in any of the analysed samples.

## 3.2. Review of literature

A detailed literature review was conducted prior to the initiation of field research. This study included many articles about geology, regional tectonics, geological structures, and stratigraphy, of lower Swat areas.

## 3.3. Field investigation

Field investigations comprised geological studies, photography of the selected rocks, and fresh bulk sampling for mechanical analysis and thin sections preparation. In geological studies different geological features were studied including grain size with the help of hand lens, differentiation of weathered surface from fresh surface, and different geological structure (e.g., augun structure, foliation in present study). Photographs were taken from different geological structure and from different varieties according to grain size.

## 3.4. Sample collection

Sample were collected from two different areas of Swat where granitic gneisses were exposed i.e., Islampur and Shir Atraf areas. In Islampur three different varieties are present, fine, medium, and coarse grain granitic gneisses. In coarse grain variety augun structures (quartzo feldspathetic gneisses) are present. The second location is Shir Atraf village where two different varieties are present, medium, and coarse grain granitic gneisses. Fresh bulk samples from each variety were collected for cores and thin sections.

## 3.5. Sample coding

The codes of the given samples have given according to rock name (Swat granitic gneisses). These codes have given to thin sections and core samples of different variety in Shir Atraf and Islampur areas. These codes are.

**SGC1** = Shir Atraf Granitic Gneisses Coarse One

**SGC2** = Shir Atraf Granitic Gneisses Coarse Two

**SGC3** = Shir Atraf Granitic Gneisses Coarse Three

**SGM1** = Shir Atraf Granitic Gneisses Medium One

**SGM2** = Shir Atraf Granitic Gneisses Medium Two

**SGM3** = Shir Atraf Granitic Gneisses Medium Three

**IGC1** = Islampur Granitic Gneisses Coarse One

**IGC2** = Islampur Granitic Gneisses Coarse Two

**IGC3** = Islampur Granitic Gneisses Coarse Three

**IGM1** = Islampur Granitic Gneisses Medium One

**IGM2** = Islampur Granitic Gneisses Medium Two

**IGM3** = Islampur Granitic Gneisses Medium Three

**IGF1** = Islampur Granitic Gneisses Fine One

**IGF2** = Islampur Granitic Gneisses Fine Two

**IGF3** = Islampur Granitic Gneisses Fine Three

## 3.6. Cores samples preparation for mechanical test

For performing UCS, UTS, water absorption and specific gravity in NCEG Geotechnical lab University of Peshawar. Core samples were prepared in Hanan technology Pakistan (pvt) limited, House 20, sector G, Ghazikot township Mansehra KPK. Cut all samples in specific length for performing mechanical tests in rock cutting lab of NCEG, University of Peshawar.

## 3.7. Laboratory work

To achieve the best results, the selected samples was subjected to a variety of laboratory techniques. For understanding mineralogical and textural features on polarizing microscope of thin sections were prepared selected rocks. In present study the laboratory work is classified into two

### 3.7.1. Geotechnical Laboratory work

The UCS, UTS, porosity, water absorption and specific gravity of the prepared core samples were performed in NCEG Geotechnical lab University of Peshawar.

### 3.7.2. Petrographic laboratory work

In petrographic laboratory work the first step is thin section preparation. Thin sections were prepared in rock cutting laboratory of Department of Geology, Bacha Khan University Charsadda.

#### a. Thin section preparation

A rock cutting machine was used to make 2 x 4cm rock chips, and one side of each chip was ground and polished to create a planer surface. The polished plane surface of the chip was then epoxy-bonded to a glass slide of the same size. Before mounting the rock chip on the glass slide, it was heated on a hot plate to temperatures above 100 C. After placing the rock chip on the glass slide, it was cut again on the rock cutting machine to reduce the thickness of the chip for further processing. The rock chip was further ground to a minimum thickness of 0.03mm using various sizes of silicon carbide powder. Cover slips were then placed over the thin sections for petrographic studies.

#### b. Thin section studies

Studied all the prepared thin sections in the petrographic laboratory of Department of Earth Sciences, Quaid I Azam Islamabad. For model minerology visual estimation technique were used and ten views of each thin section was taken. The percentage of these views have taken by simple statistical technique average.

## 3.8. Structure of thesis

**Chapter 1**

This chapter described the introduction to the current research work.

**Chapter 2**

The geological setting of the northern Indian plate in northwest Pakistan is described in this chapter. It presents the regional tectonics events (Indian Eurasian plate collision and KIA Formation) and the local stratigraphy (study area).

**Chapter 4**

This chapter described the petrography of Swat granitic gneisses of Shir Atraf and Islampur areas.

**Chapter 5**

This chapter described the results of different tests have performed. These tests include UCS, UTS, Porosity, Specific gravity, and Water absorption test.

**Chapter 6**

The importance of petrographic studies of rocks to their mechanical properties is discussed in this chapter. The different plots show the relation of petrographic studies with physical and mechanical properties of Swat granitic gneisses.

**Chapter 7**

This chapter described the discussion and conclusion of the present work.

# CHAPTER 4 PETROGRAPHY

## 4.1. General statement

A thorough understanding of modal mineralogy and textural relationships is necessary for accurate rock characterization. This information is derived from comprehensive petrographic studies of hand samples as well as thin sections. Petrographic analysis under a polarised microscope is highly useful for identifying rocks based on mineral assemblages, texture and determining the volume percentages of minerals present in rocks.

The Swat granitic gneiss is exposed in Swat and Bunir areas in north Pakistan. In this research work fifteen samples were collected from two different places in Swat i.e., Islampur and Shir Atraf areas. Thin sections observed under a polarizing microscope reveal a variety of minerals, including quartz, plagioclase, and alkali feldspar as major minerals. Minor to accessory amounts of biotite, muscovite, epidote, chlorite, tourmaline, and garnet are also present. Alkali feldspar and quartz form most of the groundmass. The modal percentage of minerals was determined by visual estimation under polarizing microscope. All these minerals were present in various proportions in all the thin sections of the studied samples. The modal mineral percentages are presented in Table 3.1. In this chapter a detailed petrographic study of the Swat granitic gneisses is given. In IUGS classification diagrams (from Le Maitre, 2002) the studied samples were plotted and shown in fig 4.24.

## 4.2. Field Investigation

Field investigations comprised geological studies, photography of the selected rocks, and fresh bulk sampling for mechanical analysis and thin sections preparation. Different geological features were examined in geological studies, including grain size using a hand lens, distinction of weathered from fresh surfaces, and different geological structures (e.g., augun structure, foliation, quartz veins, in present study). Photographs were obtained from a variety of geological structures and types based on grain size. Garnet crystals were also studied with the help of hand lens.

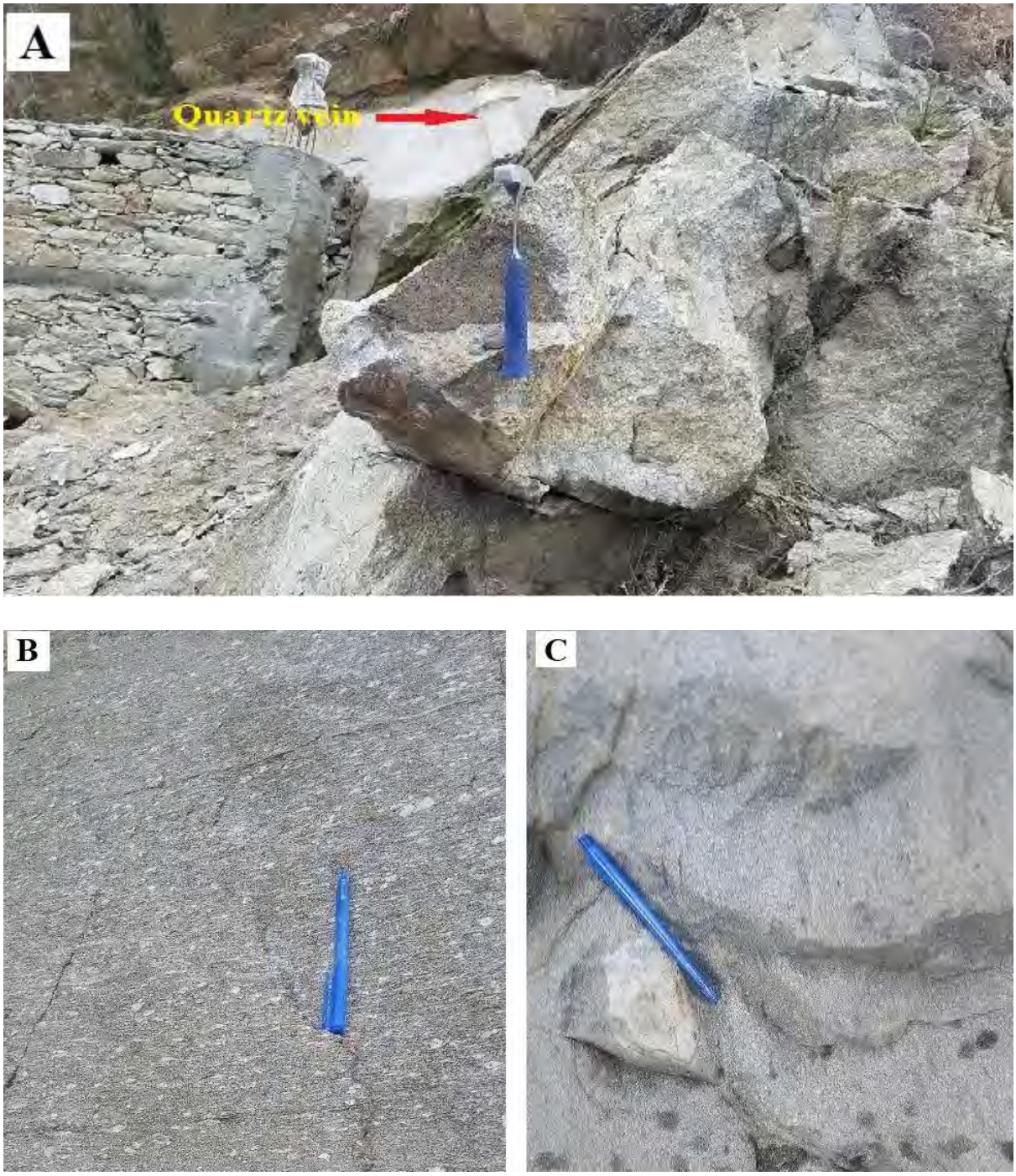


Fig. 4.1. (A) Shir Atraf granitic gneisses (B) Coarse grained variety (C) Medium grained variety

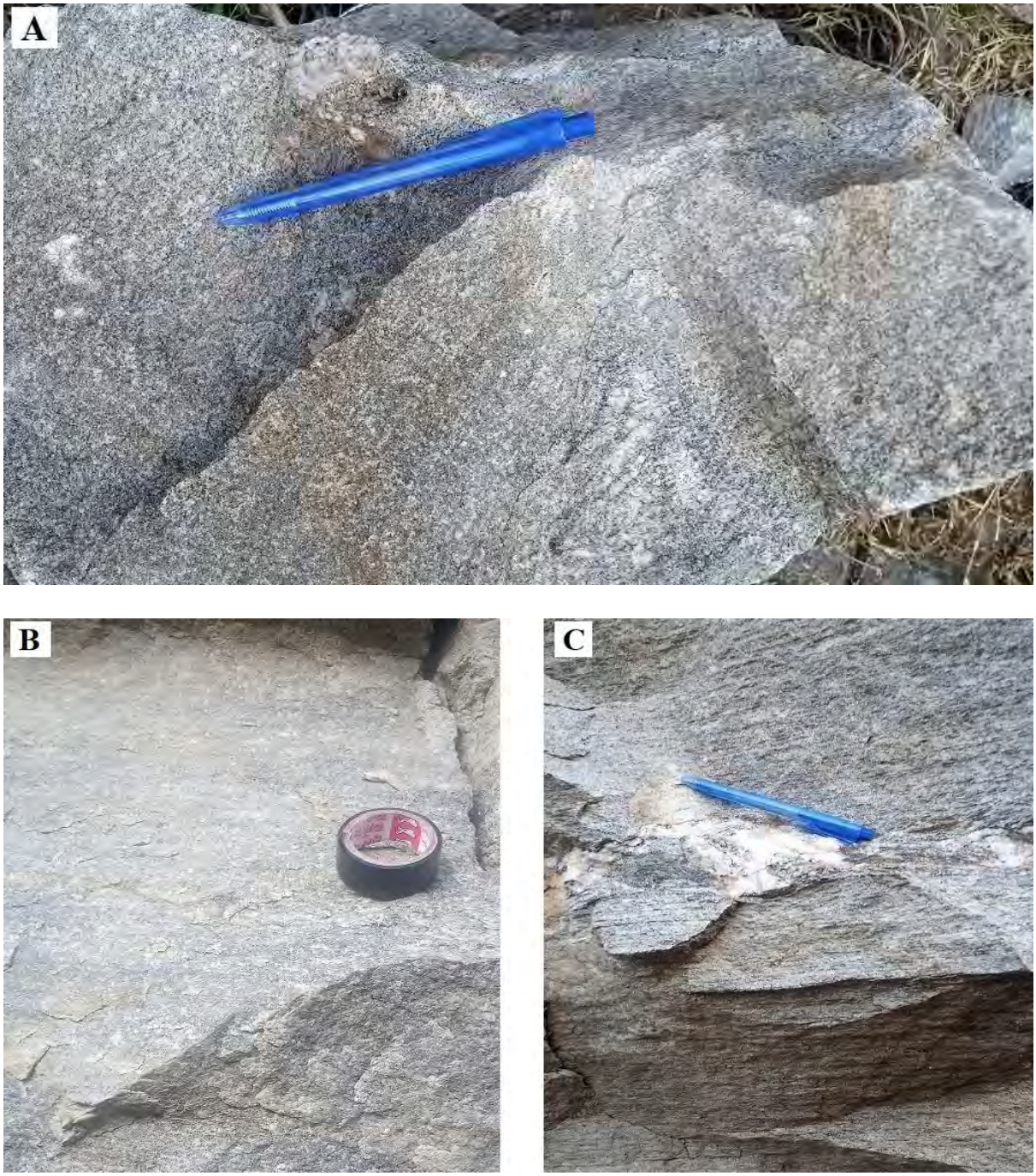


Fig. 4.2. Islampur granitic gneisses (A) Coarse grained variety (B) Medium grained variety (C) Fine grained variety

## 4.3. Petrography

Based on detailed field and petrographic observations, the rock (Swat granitic gneisses) can be grouped into two broad categories:

I. Shir Atraf granitic gneisses
II. Islampur granitic gneisses

The petrographic characteristics of these two rock groups are discussed separately below.

### 4.3.1. Shir Atraf Granitic gneisses

Texturally these rocks have two varieties, coarse and medium grained. both varieties are inequigranular and allotriomorphic in texture and contain a variety of minerals, including quartz, plagioclase, and alkali feldspar, as major minerals. Biotite, muscovite, epidote, chlorite, garnet, tourmaline, and ore minerals are also present in minor to accessory amount (Table 4.1).

#### a. Coarse grained variety

Three thin sections of coarse-grained variety were prepared for petrographic study. Minerals present in this variety are subhedral to anhedral in shape. Major mineral of order of increasing abundance are alkali feldspar (orthoclase + microcline), quartz and plagioclase. Small amount of biotite, muscovite, epidote, chlorite, garnet, tourmaline, and ore minerals are also present. All the petrographic characteristics of these minerals are discussed separately below.

**Alkali Feldspar**

In the coarse-grained variety of Shir Atraf granitic gneisses alkali feldspar is the most abundant mineral, ranging from 30% to 42% (Table 4.1). The average value of alkali feldspar in this variety is approximately 37.17%. Alkali feldspar including both orthoclase and microcline.

Microcline is present in abundant amount, occurred as a phenocryst and shows cross hatched twinning (also known as tartan twinning) (fig. 4.6b). The grains of microcline are mostly anhedral in shape. Some inclusion of quartz, biotite, and muscovite also present in it (fig. 4.6b). In some view of thin section microcline are present up to 95% (fig. 4.6b). Poikilitic and perthitic texture also present in some grains (fig. 4.6b).

Orthoclase is present in less amount as compared to microcline in this variety. These orthoclase grains are subhedral to anhedral and some grains are fractured (fig. 4.3b and 4.8b). Some inclusion of quartz also present. Poikilitic, perthitic and myrmekitic texture also present in some grains (fig. 4.4b).

**Quartz**

In this variety the quartz is the second most abundant mineral, ranging from 31% to 34%. The average value of quartz in this variety is approximately 33.3%. Most of the quartz grains are anhedral and show undulose and patchy extinction (fig. 4.3b) while some of the quartz grains are fractured.

**Plagioclase**

In this variety the plagioclase is the third most abundant mineral, ranging from 14% to 19%. The average value of plagioclase in this variety is approximately 16%. It appears in subhedral to anhedral form and shows lamellar twinning (pericline and polysynthetic twinning) (fig. 4.5b, 4.7b). It is typically surrounded by quartz and mica. Some plagioclase grains are fractured (fig. 4.4b) and having quartz inclusion (fig. 4.5b). Oscillatory zoning also occurred in some of the plagioclase grain in this variety (fig. 4.5b). plagioclase also show Carlsbad-albite twinning (fig. 4.5b).

**Muscovite**

Muscovite ranging from 3% to 6% in this variety and its average value is approximately 4.6%. Muscovite is present in flaky form, subhedral to anhedral in shape, and having perfect cleavages in some grains (fig. 4.3b, 4.4b, 4.5b, 4.7b, 4.8b). Muscovite is present in sufficient amount than biotite in this variety.

**Biotite**

Biotite ranging from 4% to 6% in this variety and the average value is approximately 5%. Biotite is brown to dark brown in colour present in the form of flakes, subhedral to anhedral in shape, and having perfect cleavages in some grains (fig. 4.4b,4.6a). Biotite is present in less amount than muscovite in this variety.

**Epidote and Chlorite**

Epidote and chlorite are present in very less amount and fine grained. Epidote ranging from 0.5% to 1% and chlorite has up to 0.5%. Finer grain size and irregular crystal growth shows that these are the product of secondary processes e.g., hydrothermal alteration. Alteration of biotite to chlorite is called chloritization and to epidote is called epidotization.

**Garnet**

Garnet is present in very less amount nearly up to 2%. Mostly garnet found with biotite, muscovite, plagioclase, and orthoclase. The grains of these garnet are mostly fractured and are anhedral in shapes (fig. 4.8).

**Tourmaline**

Tourmaline is of interest here because of its brown colours and present in very less amount nearly up to 2%. As compared to Islampur area Shir Atraf area have more tourmaline. Only the brown tourmaline is present (fig. 4.8).

**Ore Minerals**

Ore minerals are black in both plane and cross light. In this variety ore minerals are fine in size. Present in very less amount up to 1%. Mostly imbedded in other grains (quartz, alkali feldspar) (fig. 4.7b).

**Note**: in all photomicrographs: (A, PPL; B, XPL) in this chapter **Qtz** = Quartz, **Ortho** = Orthoclase, **Mic** = Microcline, **Plg** = Plagioclase, **Bt** = Biotite, **Mus** = Muscovite, **Tr** = Tourmaline, **Gr** = Garnet, **Epi** = Epidote, **Chl** = Chlorite, and **Ore M** = Ore Minerals.

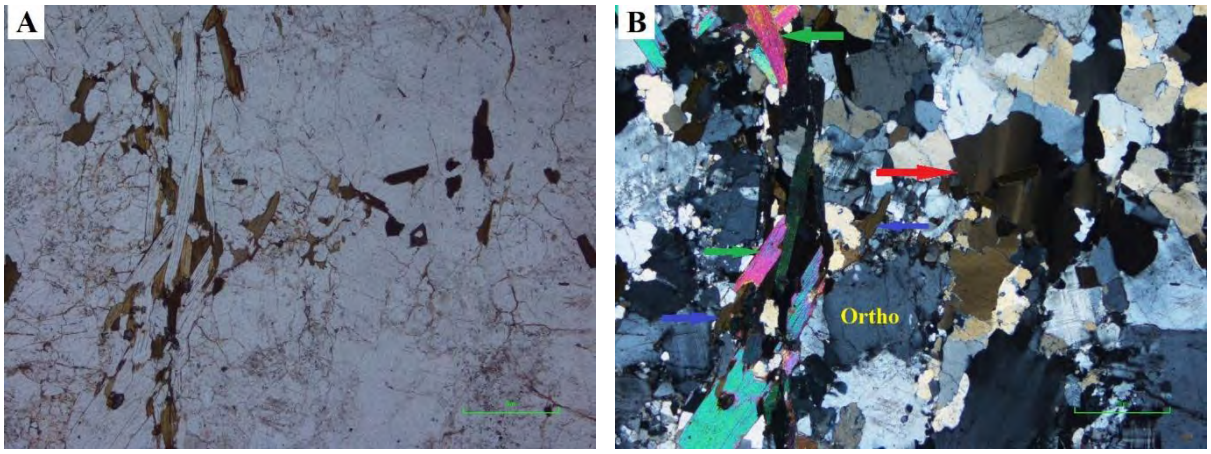


Fig. 4.3. Photomicrographs: (A, PPL; B, XPL) (B) Orthoclase, the red arrow showing undulose extinction in quartz and green arrow showing muscovite grain.

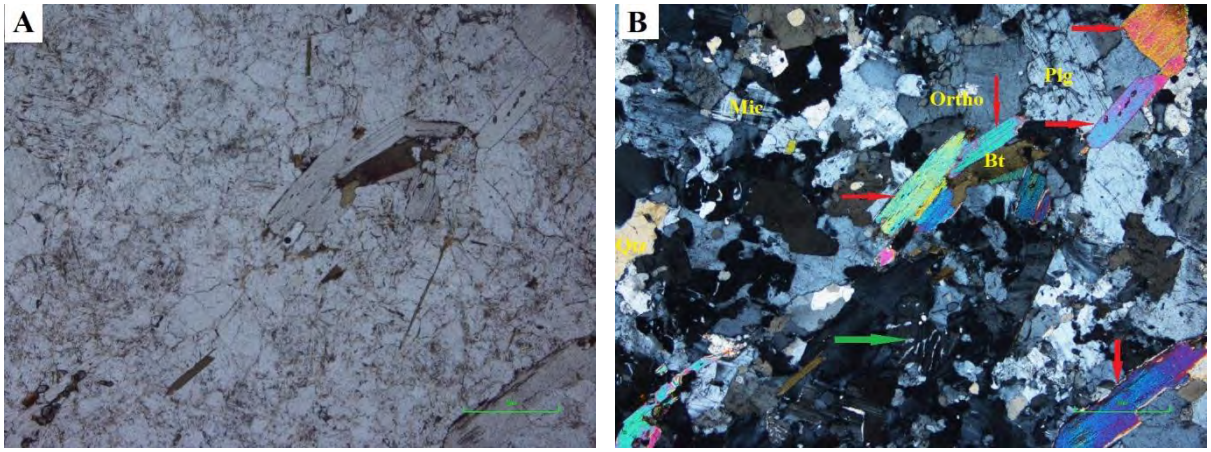


Fig. 4.4. Photomicrographs: (A, PPL; B, XPL) (B) Microcline, orthoclase, plagioclase, quartz, biotite, the red arrows showing muscovite grains and green arrow showing myrmekitic texture in orthoclase grain.

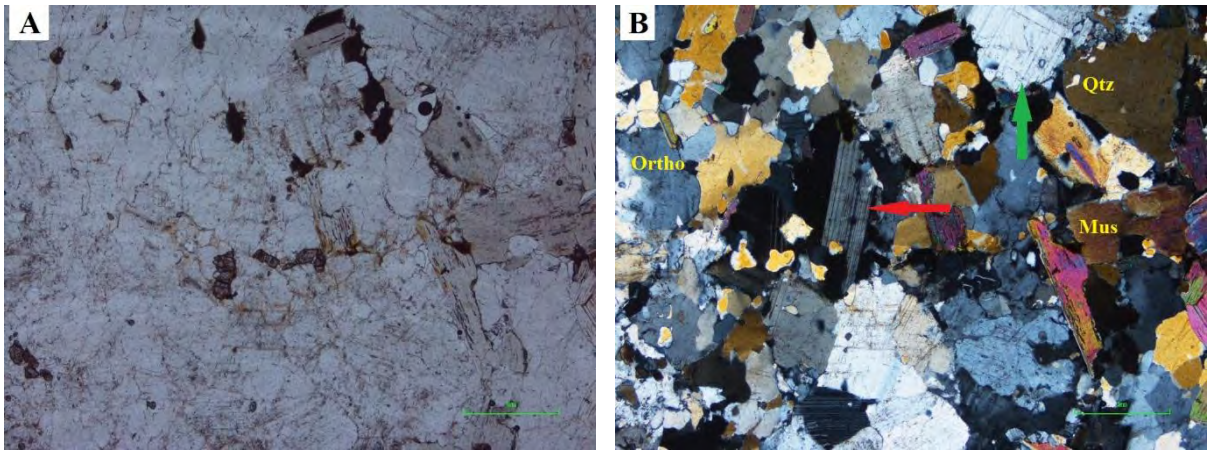


Fig. 4.5. Photomicrographs: (A, PPL; B, XPL) (B) Quartz, orthoclase, muscovite, the red arrow showing Carlsbad-albite twinning in plagioclase and green arrow showing oscillatory zoning in plagioclase grain.

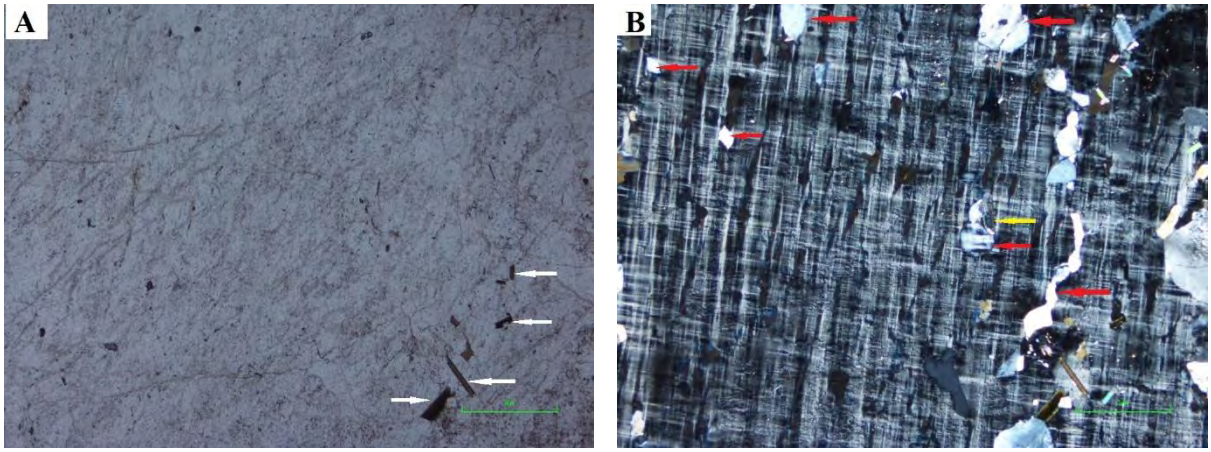


Fig. 4.6. Photomicrographs: (A, PPL; B, XPL) (A) the white arrows showing biotite grains, (B) Microcline, the red arrows showing quartz inclusion and yellow arrow showing muscovite grain inclusion in microcline.

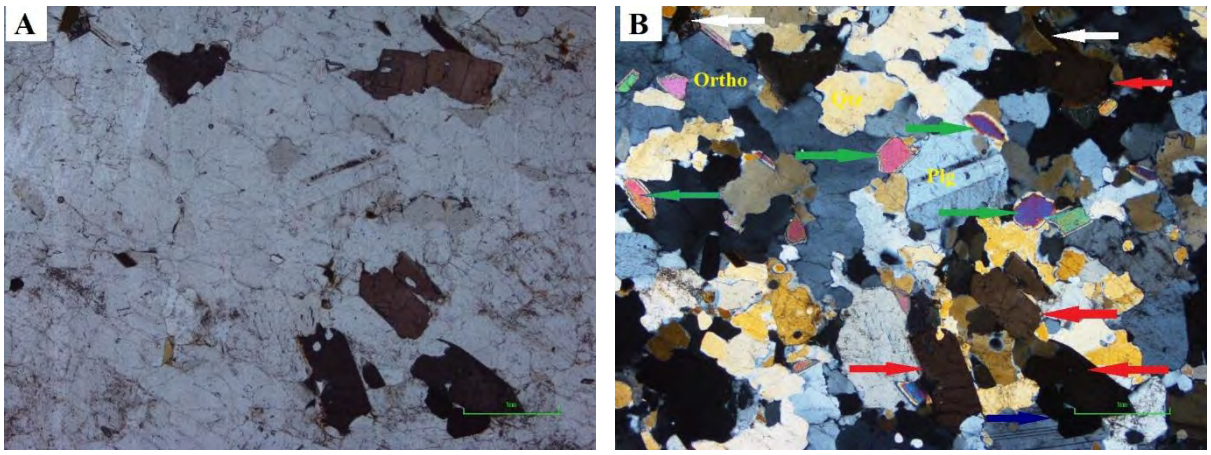


Fig. 4.7. Photomicrographs: (A, PPL; B, XPL) (A) tourmaline grains, (B) Plagioclase, orthoclase, the red arrows showing tourmaline grains, green arrows showing muscovite grains, blue arrow showing ore mineral and the white arrows showing biotite grains.

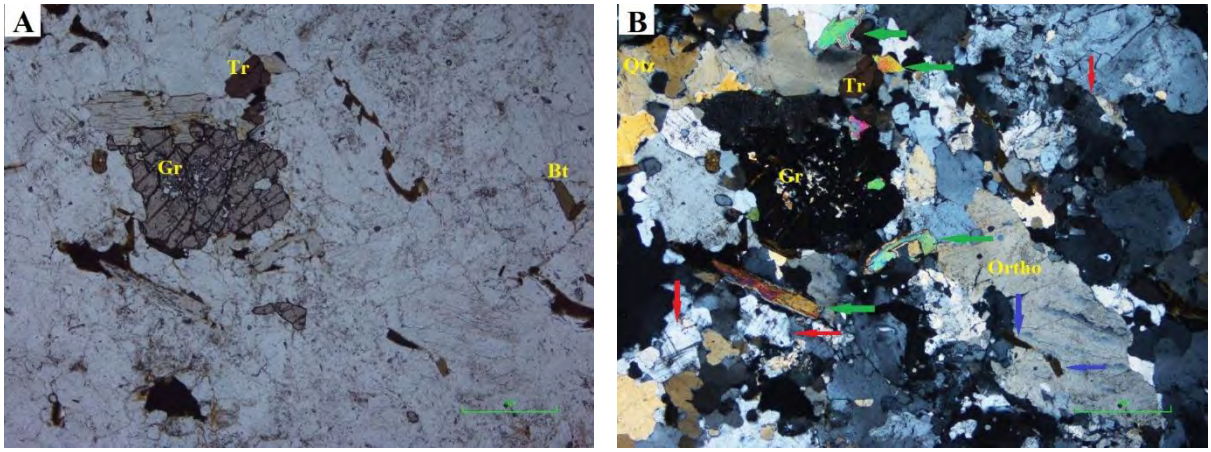


Fig. 4.8. Photomicrographs: (A, PPL; B, XPL) (A) Garnet, tourmaline, biotite grains, (B) Orthoclase, quartz, garnet, tourmaline, the blue arrows showing quartz inclusion, green arrows showing muscovite grains and red arrows showing microcline.

**b. Medium grained variety**

Three thin sections of medium-grained variety were prepared for petrographic study. Minerals present in this variety are subhedral to anhedral in shape Major mineral of order of increasing abundance are quartz, alkali feldspar (orthoclase + microcline), and plagioclase. Small amount of biotite, muscovite, epidote, chlorite, garnet, tourmaline, and ore minerals are also present. All the petrographic characteristics of these minerals are discussed separately below.

**Quartz**

In this variety the quartz is the most abundant mineral, ranging from 38% to 42% (Table 4.1). The average value of quartz in this variety is nearly 39.3%. Most of the quartz grains are anhedral, with patchy and undulose extinction (fig. 4.9b). some of the quartz grains are fractured (4.10b). Some inclusions of other minerals are also present (less amount of ore mineral).

**Alkali Feldspar**

Alkali feldspar is the second most prevalent mineral in this type, accounting for 28 to 36% of the total. The average value of alkali feldspar in this variety is approximately 31.4%. Both orthoclase and microcline found in alkali feldspar.

Orthoclase is present in greater amount as compared to microcline in this variety. These orthoclase grains are typically fractured and anhedral in shape (fig. 4.12b, 4.13b). Some

inclusion of quartz also presents (fig. 4.13b). Myrmekitic texture has been observed in some of orthoclase grains (fig. 4.13b).

Microcline is found in lower amounts and shows cross-hatched twinning (fig. 4.12b). These grains are anhedral. Quartz inclusions can also be found in some grains (fig. 4.12b).

**Plagioclase**

Plagioclase is the third most prevalent mineral in this variety, ranging from 11% to 15%. The average value of plagioclase in this variety is approximately 13%. It appears in anhedral form and shows lamellar twinning (fig. 4.11b). It's usually surrounded by quartz and mica (fig. 4.11b). Some plagioclase grains have quartz inclusions and are fractured (fig. 4.11b). Oscillatory zoning can also be found in some plagioclase grains in this variety twinning (fig. 4.11b).

**Muscovite**

Muscovite ranging from 4% to 8% in this variety and its average value is approximately 6%. Muscovite present in flaky form, subhedral to anhedral in shape, and having perfect cleavages in some grains twinning (fig. 4.9b, 4.11b, 4.13b). In this variety, muscovite is present in abundance than biotite.

**Biotite**

Biotite ranging from 4% to 6% in this variety and the average value is approximately 5%. Biotite is present in flaky form and are subhedral to anhedral in shape (fig. 4.12b, 4.13a, 4.14b). In this variety, biotite is less abundant than muscovite. Some biotite grains are altered to chlorite and epidote by chloritization and epidotization (fig. 4.10b).

**Epidote and Chlorite**

Epidote and chlorite are present in very less amount up to 1% and fine grained (fig. 4.10b). Finer grain size and irregular crystal growth indicate secondary processes, such as hydrothermal alteration. Basically, these are the alteration of biotite by chloritization and epidotization.

**Tourmaline**

Brown colours tourmaline is present in very less amount nearly up to 3%. As compared to Islampur area Shir Atraf area have more tourmaline (fig. 4.9b). Only the brown tourmaline is present (fig. 4.9).

**Garnet**

Garnet is present in very less amount nearly up to 2%. Most of the garnet is found with biotite, muscovite, and orthoclase (fig. 4.13a, 4.13b). Garnet grains are usually fractured and anhedral in shape (fig. 4.13a).

**Ore Minerals**

Ore minerals are black in both plane and cross light. Present in very less amount up to 1%. In this variety ore minerals are fine in size in some views large grain are also present. Mostly imbedded in other grains (quartz, alkali feldspar) (fig. 4.14).

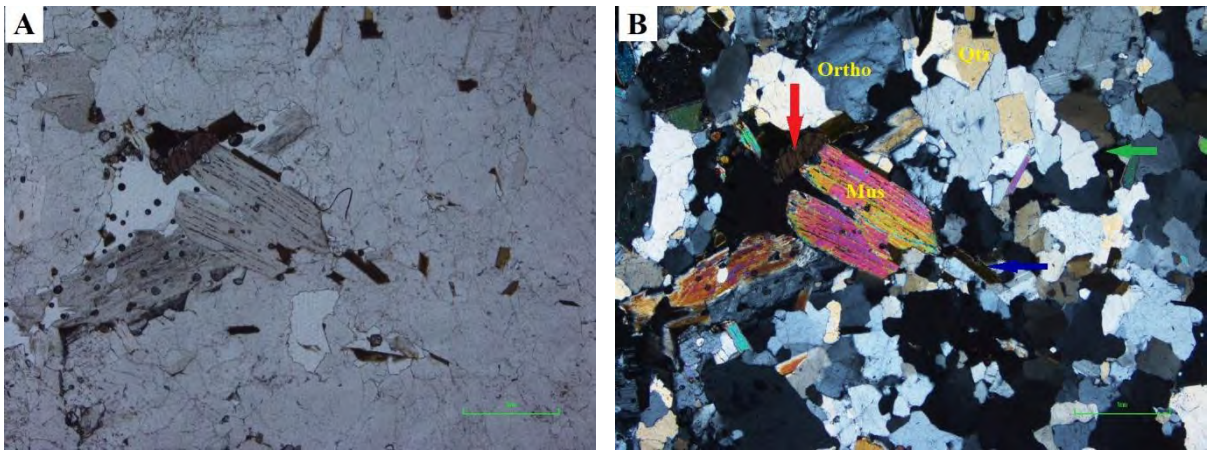


Fig. 4.9. Photomicrographs: (A, PPL; B, XPL) (B) Quartz, orthoclase, muscovite, the red arrow showing tourmaline, green arrow showing patchy extinction in quartz grain and blue arrow showing biotite grain.

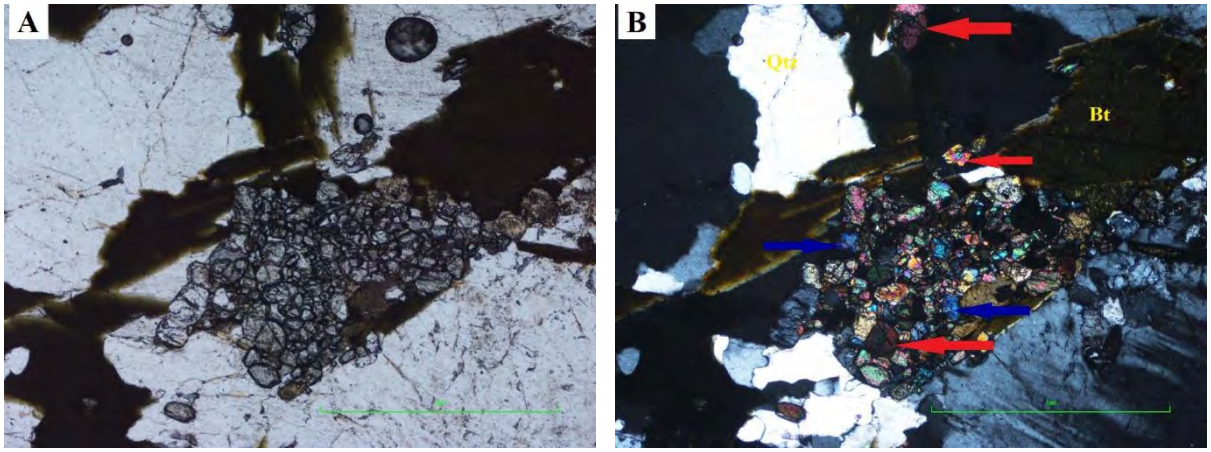


Fig. 4.10. Photomicrographs: (A, PPL; B, XPL) (B) Quartz, biotite, the red arrows showing epidote and blue arrows showing chlorite.

Note: all the other photomicrographs have taken in 2x lens, but 4.10 photomicrograph taken in 5x lens because epidote and chlorite grains are very fine.

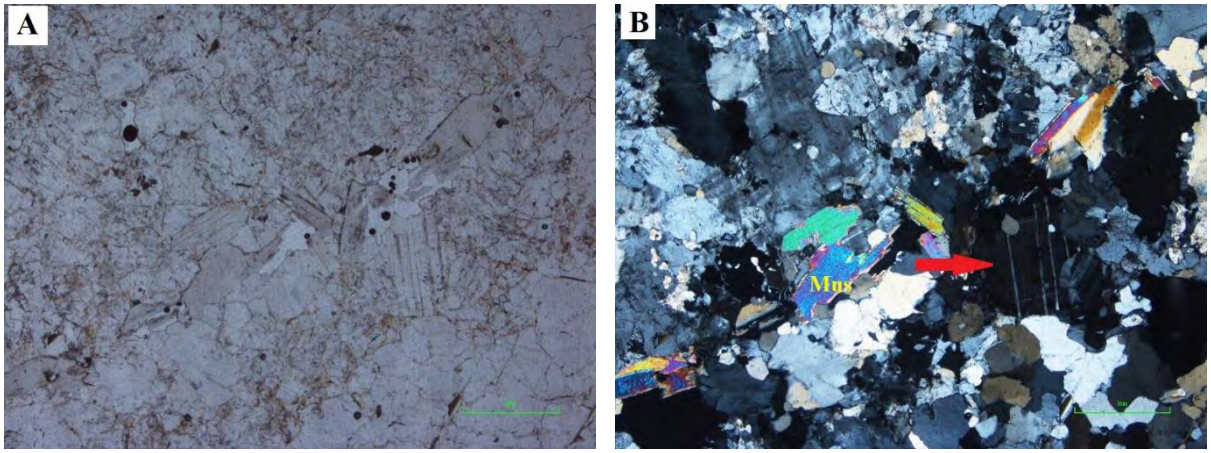


Fig. 4.11. Photomicrographs: (A, PPL; B, XPL) (B) Muscovite, the red arrows showing oscillatory zoning in plagioclase grain.

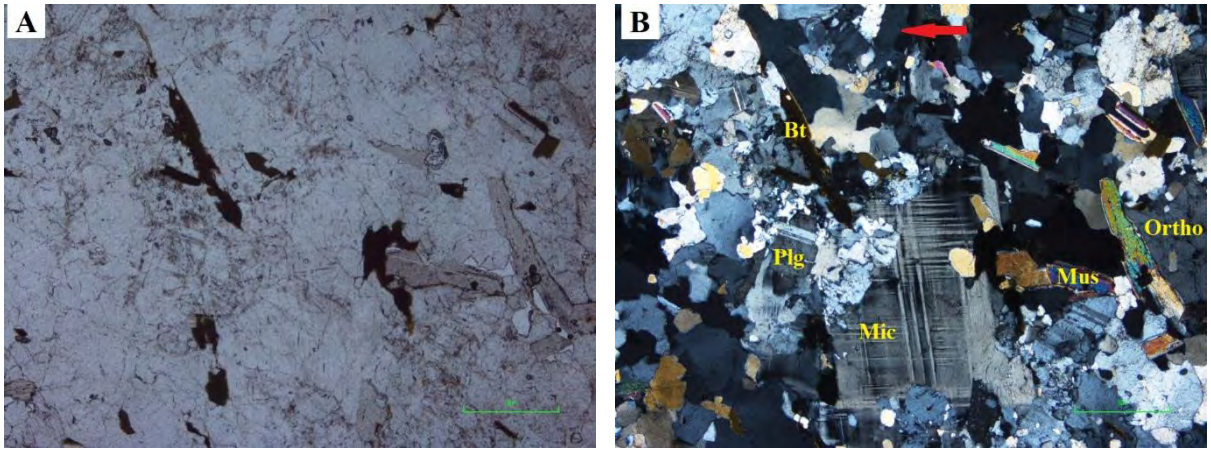


Fig. 4.12. Photomicrographs: (A, PPL; B, XPL) (B) Orthoclase, plagioclase, microcline, muscovite, biotite, the red arrow showing patchy extinction in quartz grain.

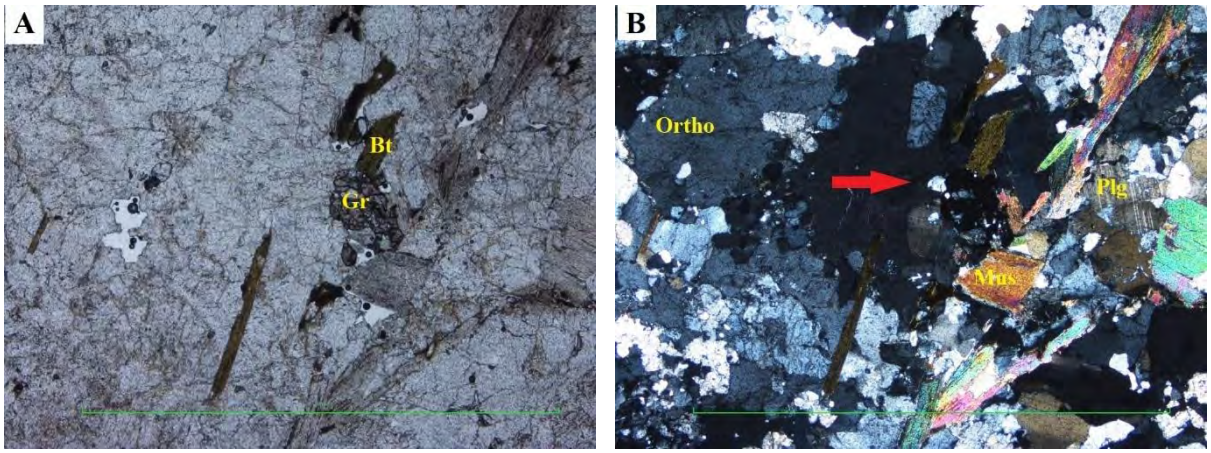


Fig. 4.13. Photomicrographs: (A, PPL; B, XPL) (A) Garnet, biotite (B) Orthoclase, plagioclase, muscovite, the red arrow showing poikilitic texture in orthoclase grain.

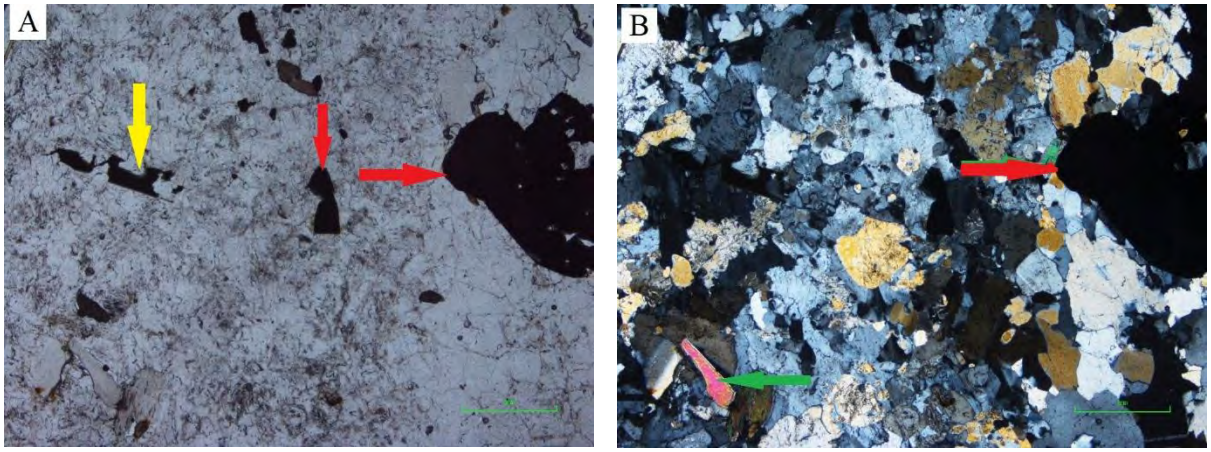


Fig. 4.14. Photomicrographs: (A, PPL; B, XPL) (A) the red arrows showing the ores grains, the yellow arrow showing biotite (B) green arrows showing muscovite grains.

### 4.3.2. Islampur Granitic gneisses

Texturally Islampur granitic gneisses have three varieties, coarse, medium, and fine grained. All these varieties are inequigranular and allotriomorphic in texture. Thin sections observation under a microscope reveals a variety of minerals, including quartz, plagioclase, and alkali feldspar is major minerals, while biotite, muscovite, epidote, chlorite, garnet, tourmaline, and ore minerals are present in accessory to minor amount.

#### c. Coarse grained variety

Three thin sections of coarse-grained variety were prepared for petrographic study. Minerals present in this variety are subhedral to anhedral in shape. Major mineral of order of increasing abundance are alkali feldspar (orthoclase + microcline), quartz and plagioclase. Small amount of biotite, muscovite, epidote, chlorite, and ore minerals are also present. All the petrographic characteristics of these minerals are discussed separately below.

**Alkali Feldspar**

In this variety the alkali feldspar is the most abundant mineral, ranging from 35% to 42%. The average value of alkali feldspar in this variety is approximately 38.5%. Both microcline and orthoclase are observed in thin sections.

Microcline is present in abundant amount, shows cross hatched twinning (also known as tartan twinning) and anhedral in shape (fig. 4.17b). In some view of thin sections microcline are present up to 95% (fig. 4.17b). Some of the microcline grains have inclusion of quartz (fig. 4.17b).

Orthoclase is present in less amount as compared to microcline in this variety. These orthoclase grains are subhedral to anhedral and some grains are fractured (fig. 4.15a). Some inclusions of other minerals (quartz, biotite, and muscovite) are also present (4.18b). Some of the grains show poikilitic texture (fig. 4.18b).

**Quartz**

In this variety the quartz is the second most abundant mineral, ranging from 36% to 40%. The average value of quartz in this variety is approximately 38%. Most of the quartz grains are anhedral and show undulose and patchy extinction also present (fig. 4.16b). Most of the quartz are fractured. Some inclusion of biotite may also present (fig. 4.16b).

**Plagioclase**

In this variety the plagioclase is the third most abundant mineral, ranging from 8% to 12%. The average value of plagioclase in this variety is approximately 10%. It appears in subhedral to anhedral form and shows lamellar twinning and surrounded by quartz and orthoclase (fig. 4.18b).

**Biotite**

Biotite ranging from 4% to 9% in this variety and the average value is approximately 6%. Biotite is brown to dark brown in colour and are in tabular form. It appears as euhedral to subhedral in shape (fig. 4.15a b, 4.17a). Biotite is present in sufficient amount than muscovite in this variety.

**Muscovite**

Muscovite ranging from 4% to 8% in this variety and its average value is approximately 5.5%. Muscovite present in flaky form, subhedral to anhedral in shape, and having perfect cleavages in some grains (fig. 4.15b, 4.18b). Muscovite is present in less amount than biotite in this variety.

**Epidote and Chlorite**

Epidote and chlorite are present in very less amount and fine grained (fig. 4.15b). Epidote ranging from 1% to 2% and chlorite is up to 1%. Finer grain size and irregular crystal growth shows that these are the product of secondary processes e.g., hydrothermal alteration.

**Ore Minerals**

Ore minerals are black in both plane and cross light. In this variety ore minerals are fine in size. Present in very less amount up to 1%. Mostly imbedded in other grains (quartz, alkali feldspar) (fig. 4.17a).

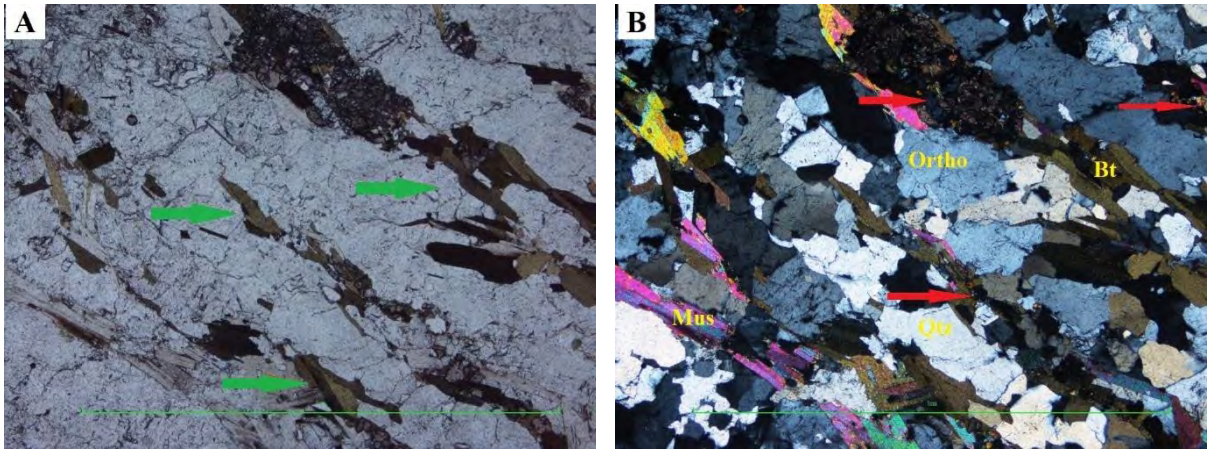


Fig. 4.15. Photomicrographs: (A, PPL; B, XPL) (A) the green arrows showing biotite grains (B) Orthoclase, muscovite, biotite, the red arrows showing biotite ultration to epidote and chlorite.

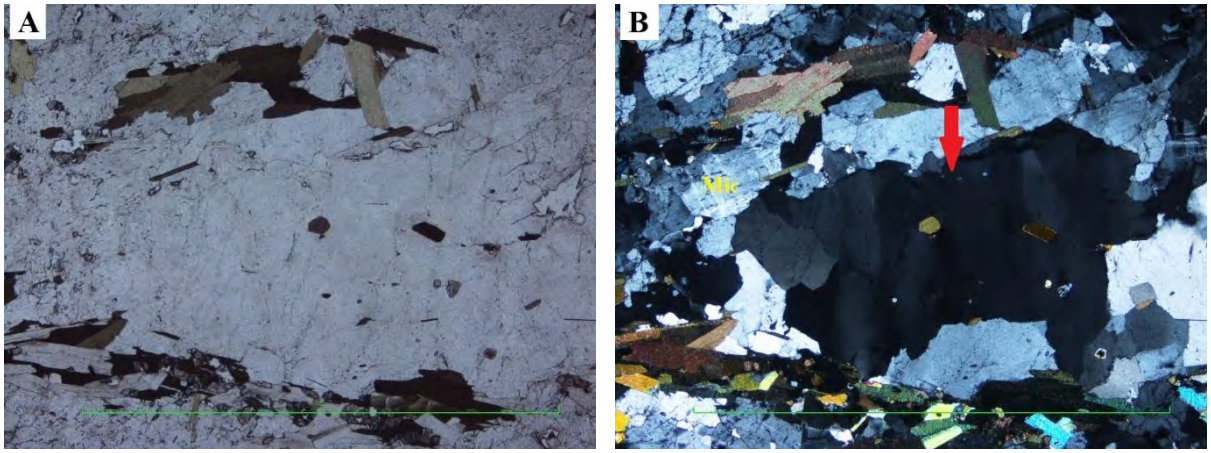


Fig. 4.16. Photomicrographs: (A, PPL; B, XPL) (B) Microcline, the red arrow showing undulose extinction in quartz (inclusion of biotite also present).

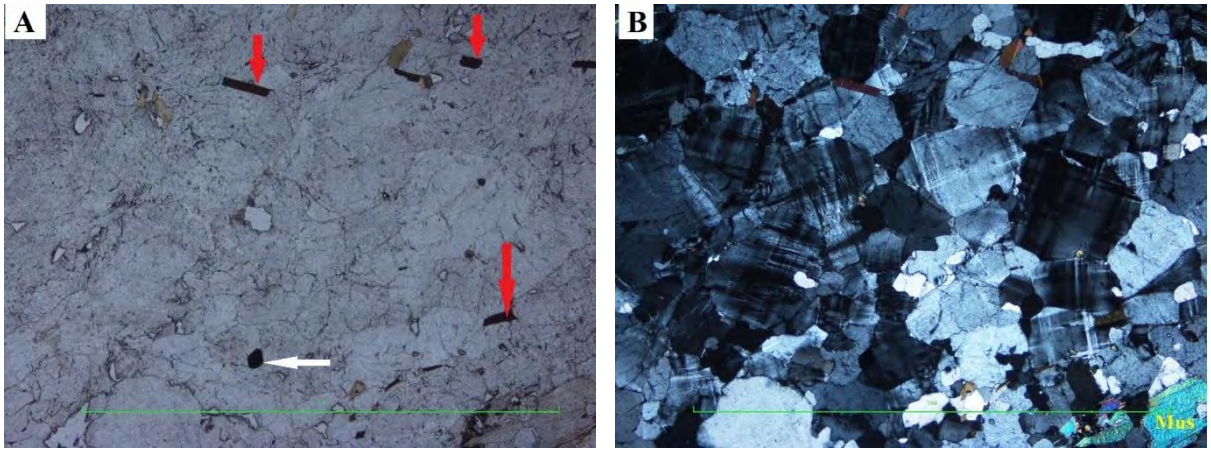


Fig. 4.17. Photomicrographs: (A, PPL; B, XPL) (A) white arrow showing ore grain, red arrows showing biotite grains (B) many microcline grains, muscovite.

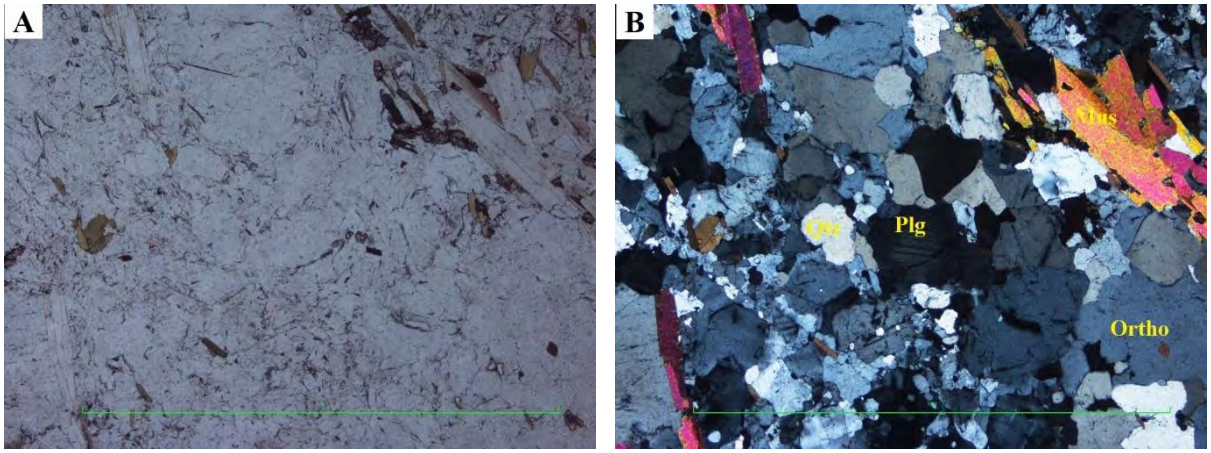


Fig. 4.18. Photomicrographs: (A, PPL; B, XPL) (B) Orthoclase, quartz, plagioclase, muscovite.

### d. Medium grained variety

Three thin sections of medium-grained variety were prepared for petrographic study. Minerals present in this variety are subhedral to anhedral in shape. The grains were comparatively small as compared to coarse grain. Major mineral of order of increasing abundance are quartz, alkali feldspar (orthoclase + microcline), and plagioclase. Small amount of biotite, muscovite, epidote, chlorite, garnet, tourmaline, and ore minerals are also present. All the petrographic characteristics of these minerals are discussed separately below.

**Quartz**

In this variety the quartz is the most abundant mineral, ranging from 34% to 40%. The average value of quartz in this variety is approximately 37.6%. This variety contain more poly

crystalline quartz as compared to coarse grain variety of Islampur granitic gneisses. Most of the quartz grains are anhedral, show undulose and patchy extinction (fig. 4.21b). Some grains of the quartz are fractured (fig. 4.21b). Quartz grains are mostly interlocked with each other (fig. 4.21b).

**Alkali Feldspar**

In this variety the alkali feldspar is the second most abundant mineral, ranging from 28% to 35%. The average value of alkali feldspar in this variety is approximately 28.1%. Alkali feldspar including both orthoclase and microcline.

Microcline is present in abundant amount and shows cross hatched twinning (also known as tartan twinning) (fig. 4.23b). Some of the grains occurred as a phenocryst and these grains are subhedral to anhedral (4.23b).

Orthoclase is present in less amount as compared to microcline in this variety. These orthoclase grains are subhedral to anhedral (fig. 4.19b, 4.21b, 4.22b). Some inclusion of quartz and biotite is also present. Perthitic and poikilitic texture in some orthoclase grains are also present (fig. 4.19b 4.23b).

**Plagioclase**

In this variety plagioclase is the third most abundant mineral, ranging from 16% to 27%. The average value of plagioclase is approximately 21.5%. It appears in subhedral to anhedral form and shows lamellar twinning and mostly surrounded by quartz and mica (fig. 4.19b, 4.20b, 4.21b). Carlsbad-albite twinning is also present in some grains (fig. 4.20b) Some plagioclase grains are fractured and having quartz inclusion (fig. 4.19b, 4.21b).

**Biotite**

Biotite ranging from 5% to 8% in this variety and the average value is approximately 6.5%. Biotite is brown to dark brown in colour and is in tabular form (fig. 4.22b, 4.23b). It appears as euhedral to subhedral in shape (fig. 4.22b, 4.23b). Biotite is present in sufficient amount than muscovite in this variety. Some biotite grains altered to epidote and chlorite (fig. 4.22b).

**Muscovite**

Muscovite ranging from 3% to 6% in this variety and its average value is approximately 4.75%. Muscovite is present in flaky form, and subhedral to anhedral in shape (fig. 4.19b, 4.21b). Muscovite is present in less amount than biotite in this variety.

**Epidote and Chlorite**

Epidote and chlorite are present in very less amount and fine grained (fig. 4.19a). Epidote and chlorite present up to 1%. Finer grain size and irregular crystal growth shows that these are the product of secondary processes e.g., hydrothermal alteration.

**Garnet**

Garnet is present in very less amount nearly up to 0.5%. In Islampur area only this variety contain garnet and tourmaline. Mostly garnet found with biotite, muscovite, and orthoclase (fig. 4.19b). The grains of these garnet are mostly fractured and are anhedral in shapes (fig. 4.19a).

**Tourmaline**

Tourmaline is of interest here because of its brown colours and present in very less amount nearly up to 0.5% (fig. 4.20b). In Islampur area only this variety contain garnet and tourmaline.

**Ore Minerals**

Ore minerals are black in both plane and cross light. In this variety ore minerals are fine in size. Present in very less amount up to 1%. Mostly imbedded in other grains (quartz, alkali feldspar).

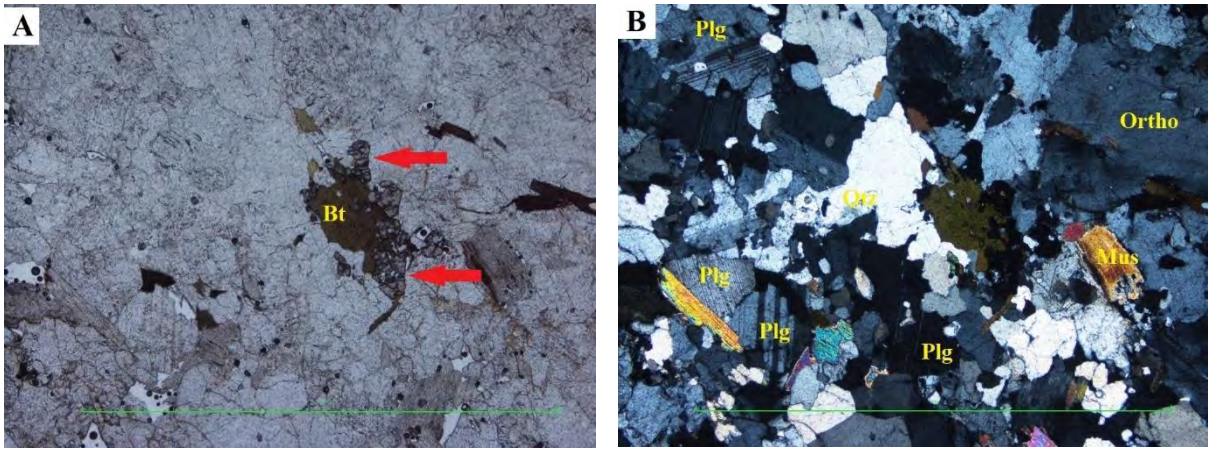


Fig. 4.19. Photomicrographs: (A, PPL; B, XPL) (A) Biotite, the red arrows showing garnet grains (B) Orthoclase, quartz, plagioclase, muscovite.

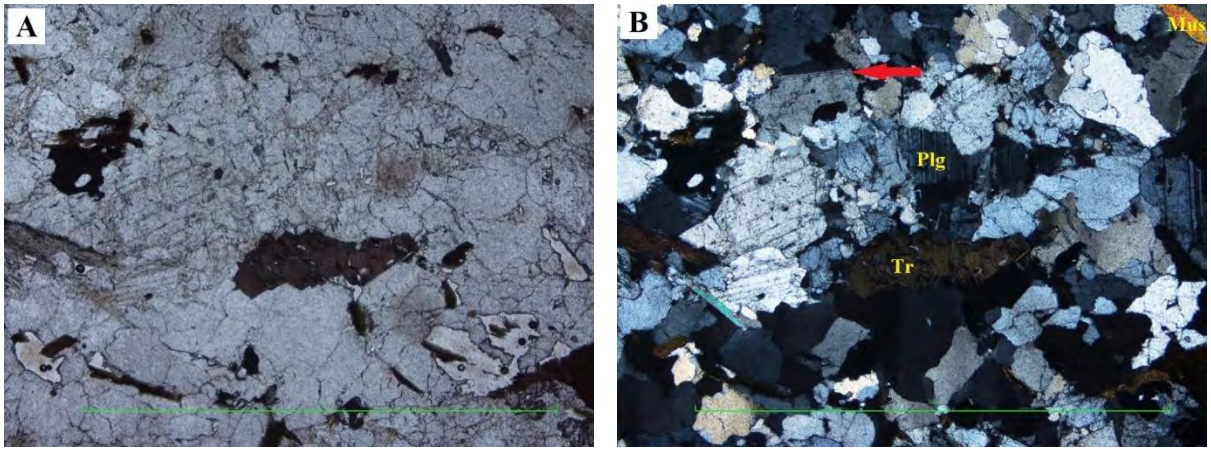


Fig. 4.20. Photomicrographs: (A, PPL; B, XPL) (A) brown tourmaline (B) plagioclase, muscovite, the red arrows showing Carlsbad-albite twinning in plagioclase.

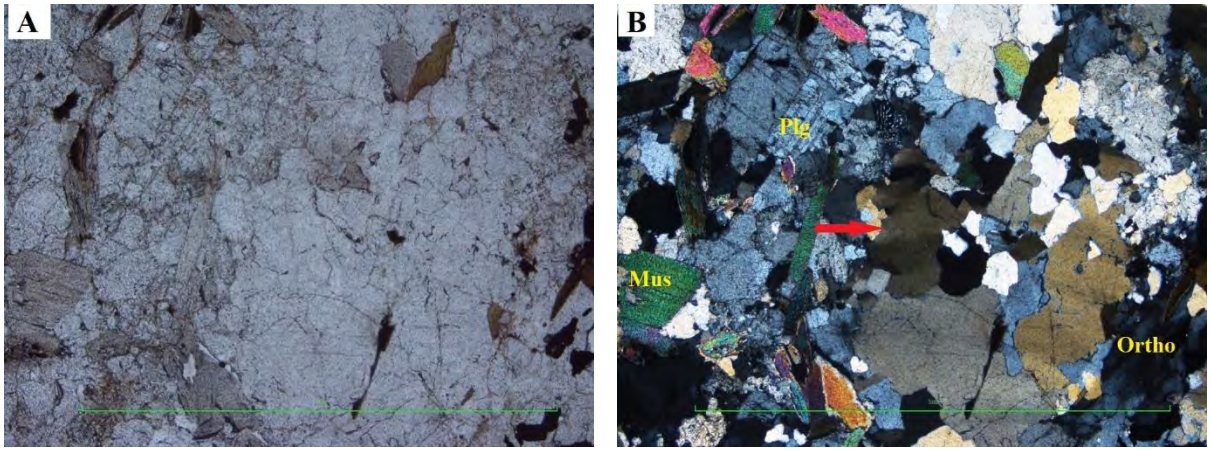


Fig. 4.21. Photomicrographs: (A, PPL; B, XPL) (B) Plagioclase, orthoclase, muscovite, the red arrow showing undulose extinction in quartz.

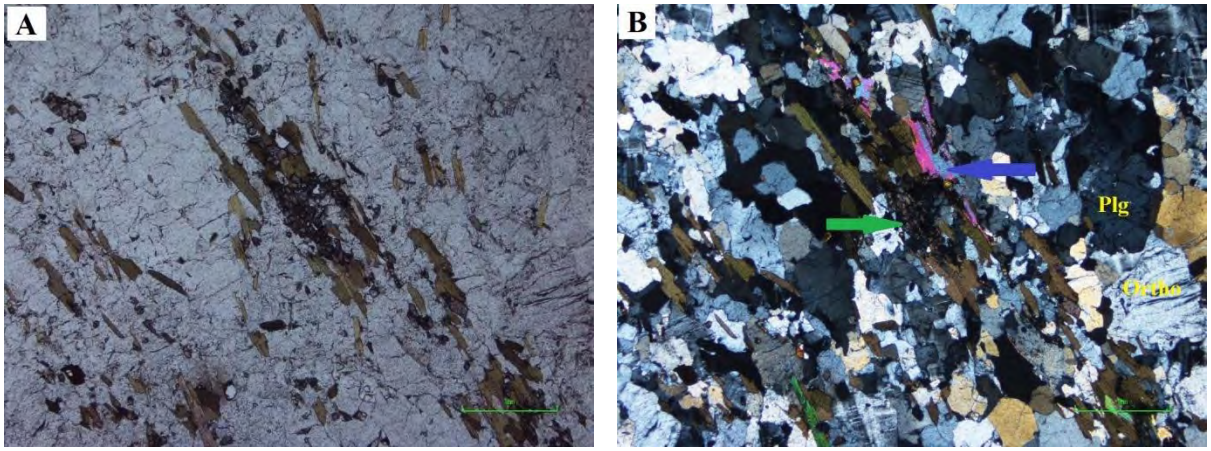


Fig. 4.22. Photomicrographs: (A, PPL; B, XPL) (B) orthoclase (perthitic texture), plagioclase, the green arrow showing biotite ultration to epidote and chlorite, the blue arrow showing muscovite.

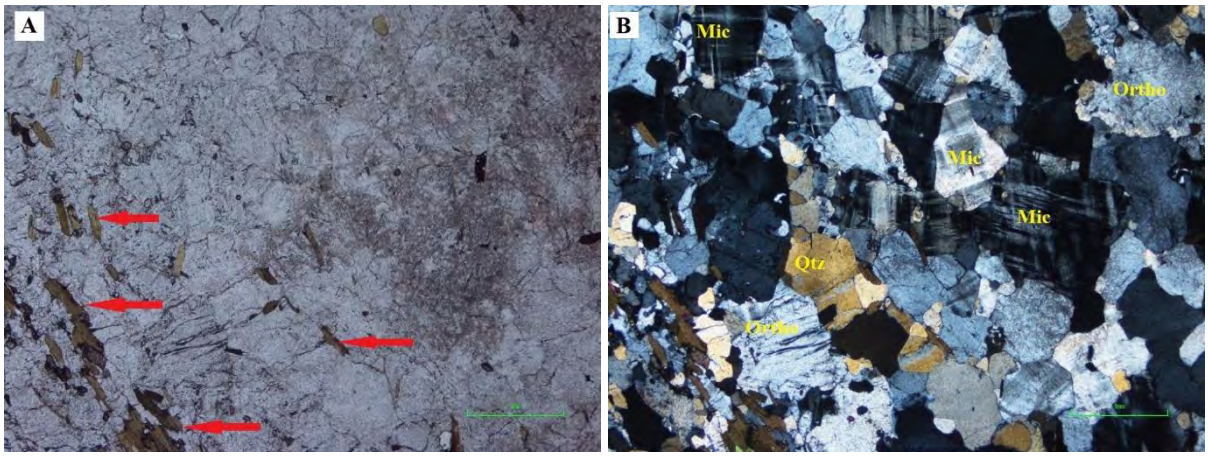


Fig. 4.23. Photomicrographs: (A, PPL; B, XPL) (A) The red arrows showing biotite grains (B) Microcline, orthoclase (perthitic texture) and quartz.

### e. Fine grained variety

Three thin sections of Fine-grained variety were prepared for petrographic study. Minerals present in this variety are subhedral to anhedral in shape. The grains were comparatively small as compared to medium and coarse-grained varieties. Major mineral of order of increasing abundance are quartz, alkali feldspar (orthoclase + microcline), and plagioclase. Small amount of biotite, muscovite, and ore minerals are also present. All the petrographic characteristics of these minerals are discussed separately below.

**Quartz**

In this variety the quartz is the most abundant mineral, ranging from 41% to 45%. The average value of quartz in this variety is approximately 42.5%. This variety contain more poly crystalline quartz as compared to other two varieties of Islampur granitic gneisses. Most of the quartz grains are subhedral to anhedral, shows undulose and patchy extinction (4.24b). This variety mostly grounded by quartz (fig. 4.24, 4.25, 4.26).

**Alkali Feldspar**

In this variety the alkali feldspar is the second most abundant mineral, ranging from 31% to 35%. The average value of alkali feldspar in this variety is approximately 32.95%. Alkali feldspar including both orthoclase and microcline.

Orthoclase is present in abundant amount as compared to microcline in this variety. These orthoclase grains are subhedral to anhedral (fig. 4.24b, 4.25b, 4.26b). Orthoclase grains are large as compared to other minerals of this variety (fig. 4.25b). Some inclusions of other minerals (quartz) are also present (fig. 4.26b). Myrmekitic texture is also present in some grains (fig. 4.25b).

Microcline is present in less amount and shows cross hatched twinning (also known as tartan twinning) and is subhedral to anhedral in shape (fig. 4.24b, 4.26b). Some inclusion of quartz also occurred (fig. 4.24b).

**Plagioclase**

In this variety plagioclase is the third most abundant mineral, ranging from 14% to 16%. The average value of plagioclase is approximately 15.4%. It appears in anhedral form, shows lamellar twinning mostly surrounded by quartz (fig. 4.24b, 4.26b).

**Biotite**

Biotite ranging from 5% to 6% in this variety and the average value is approximately 5.8%. Biotite is brown to dark brown in colour and are in tabular form. Some grains are present in needle form (fig. 4.24a). It appears as euhedral to subhedral in shape (fig. 4.24, 4.26). Biotite is present in sufficient amount than muscovite in this variety.

**Muscovite**

Muscovite ranging from 2% to 5% in this variety and its average value is approximately 3.1%. Muscovite present in flaky form, and subhedral to anhedral in shape (fig. 4.25b). Muscovite is present in less amount than biotite in this variety.

**Ore Minerals**

Ore minerals are black in both plane and cross light. In this variety ore minerals are fine in size (fig. 4.25a). Present in very less amount up to 1%. Mostly imbedded in other grains (quartz, alkali feldspar) (fig. 4.26b).

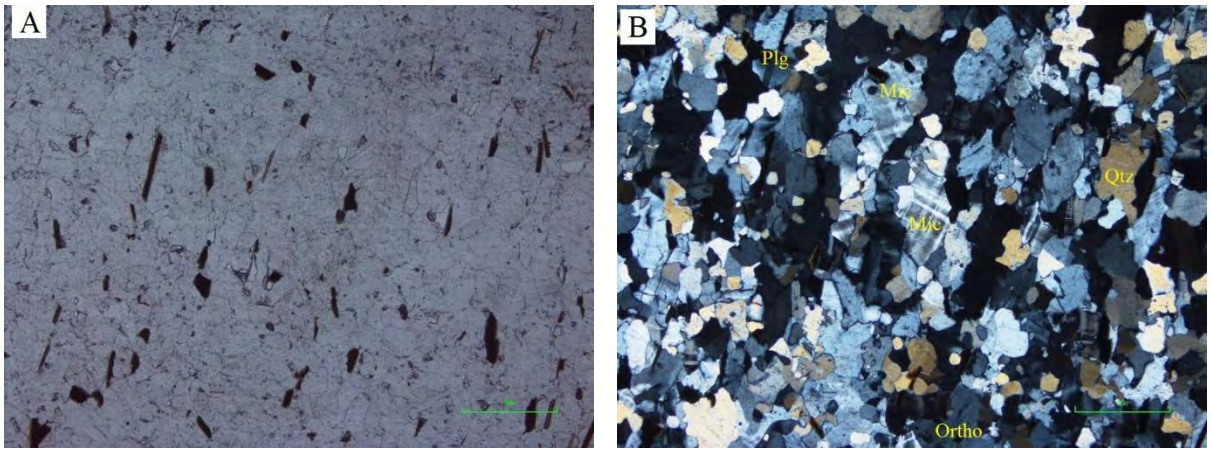


Fig. 4.24. Photomicrographs: (A, PPL; B, XPL) (A) Biotite (some grains in needle form), some fine ore grains (B) Quartz (polycrystalline), orthoclase, plagioclase, microcline.

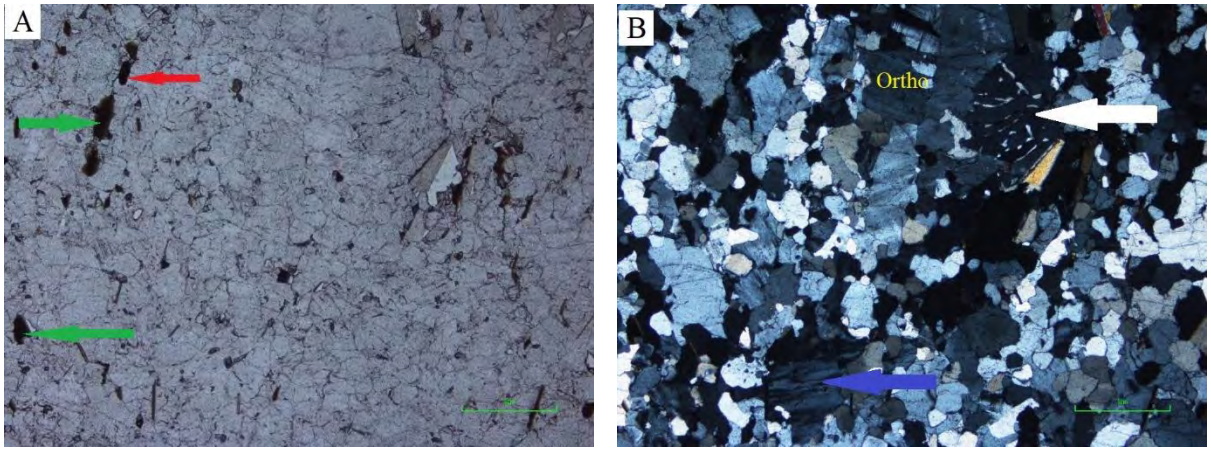


Fig. 4.25. Photomicrographs: (A, PPL; B, XPL) (A) the red arrow showing ore grain, the green arrows showing biotite grains. (B) orthoclase (quartz inclusion are present), the white arrow showing Myrmekitic texture in orthoclase grain, the blue arrow showing perthitic texture in orthoclase grain.

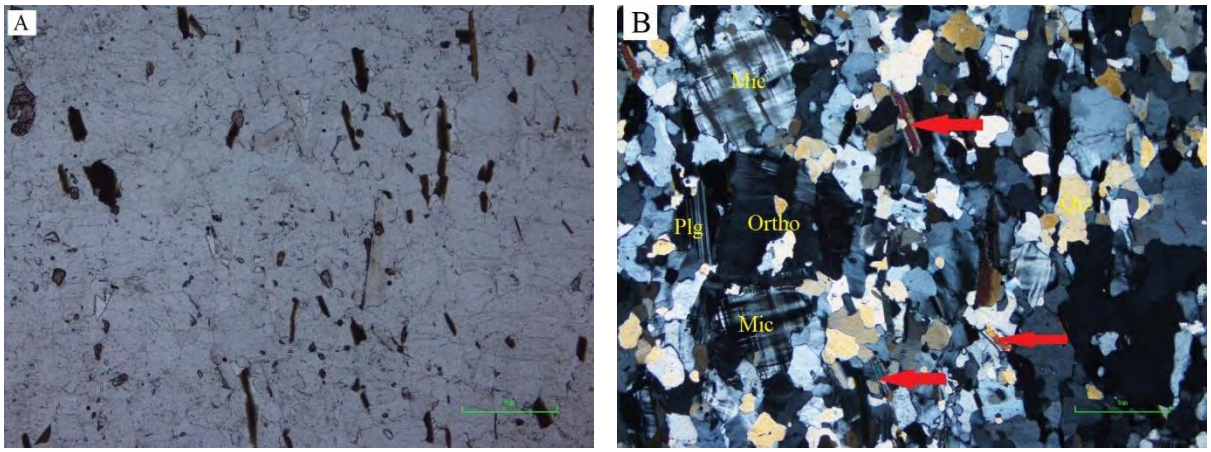


Fig. 4.26. Photomicrographs: (A, PPL; B, XPL) (B) Quartz (polycrystalline), orthoclase (quartz inclusion are present), plagioclase, microcline, the red arrows showing muscovite grains.

**Table 4.1.** Modal composition of Shir Atraf and Islampur granitic gneisses

| S.No | Quartz | Alk.F | Plg | Mus | Bt | Gr | Tr | Epi | Chl | Ore M |
|---|---|---|---|---|---|---|---|---|---|---|
| **SGC1** | 31.4 | 40.3 | 14 | 6 | 5.3 | 2 | -- | 1 | 0.3 | -- |
| **SGC2** | 33 | 39 | 15 | 6 | 4 | 2 | 1 | -- | -- | -- |
| **SGC3** | 33.5 | 30 | 18.8 | 3.5 | 5.5 | 3 | 3 | 1 | 0.7 | 1 |
| **SGM1** | 38 | 31 | 14.5 | 6 | 5 | 1.5 | 1.5 | 1 | 0.5 | 1 |
| **SGM2** | 42 | 28.5 | 13.5 | 4.5 | 5.5 | 1 | 3 | 1 | 1 | -- |
| **SGM3** | 38 | 34.5 | 11 | 7.2 | 4.3 | 1 | 2 | 1 | 0.5 | 0.5 |
| **IGC1** | 37 | 35.5 | 10.5 | 7 | 7 | -- | -- | 2 | 1 | -- |
| **IGC2** | 36 | 41.5 | 8.5 | 4 | 8.5 | -- | -- | 0.5 | 0.5 | 0.5 |
| **IGC3** | 39.5 | 35 | 11.5 | 7.4 | 4.2 | -- | -- | 1 | 0.5 | 1 |
| **IGM1** | 40.3 | 28.2 | 16 | 6 | 7 | 1 | -- | 0.5 | 0.5 | 0.5 |
| **IGM2** | 34.8 | 28 | 27 | 3.5 | 5 | 0.5 | 0.2 | 0.5 | -- | 0.5 |
| **IGM3** | 33 | 35 | 18 | 5 | 7.6 | -- | 0.4 | 0.5 | 0.5 | -- |
| **IGF1** | 45 | 31.5 | 14.8 | 2.2 | 5.5 | -- | -- | -- | -- | 1 |
| **IGF2** | 41 | 35 | 16 | 3 | 5 | -- | -- | -- | -- | -- |
| **IGF3** | 39.8 | 34.5 | 15 | 4.2 | 6 | -- | -- | -- | -- | 0.5 |

**Note**: **Qtz** = Quartz, **Alk.F** = Alkali feldspar including orthoclase and microcline, **Plg** = Plagioclase, **Bt** = Biotite, **Mus** = Muscovite, **Tr** = Tourmaline, **Gr** = Garnet, **Epi** = Epidote, **Chl** = Chlorite, **Ore M** = Ore Minerals.

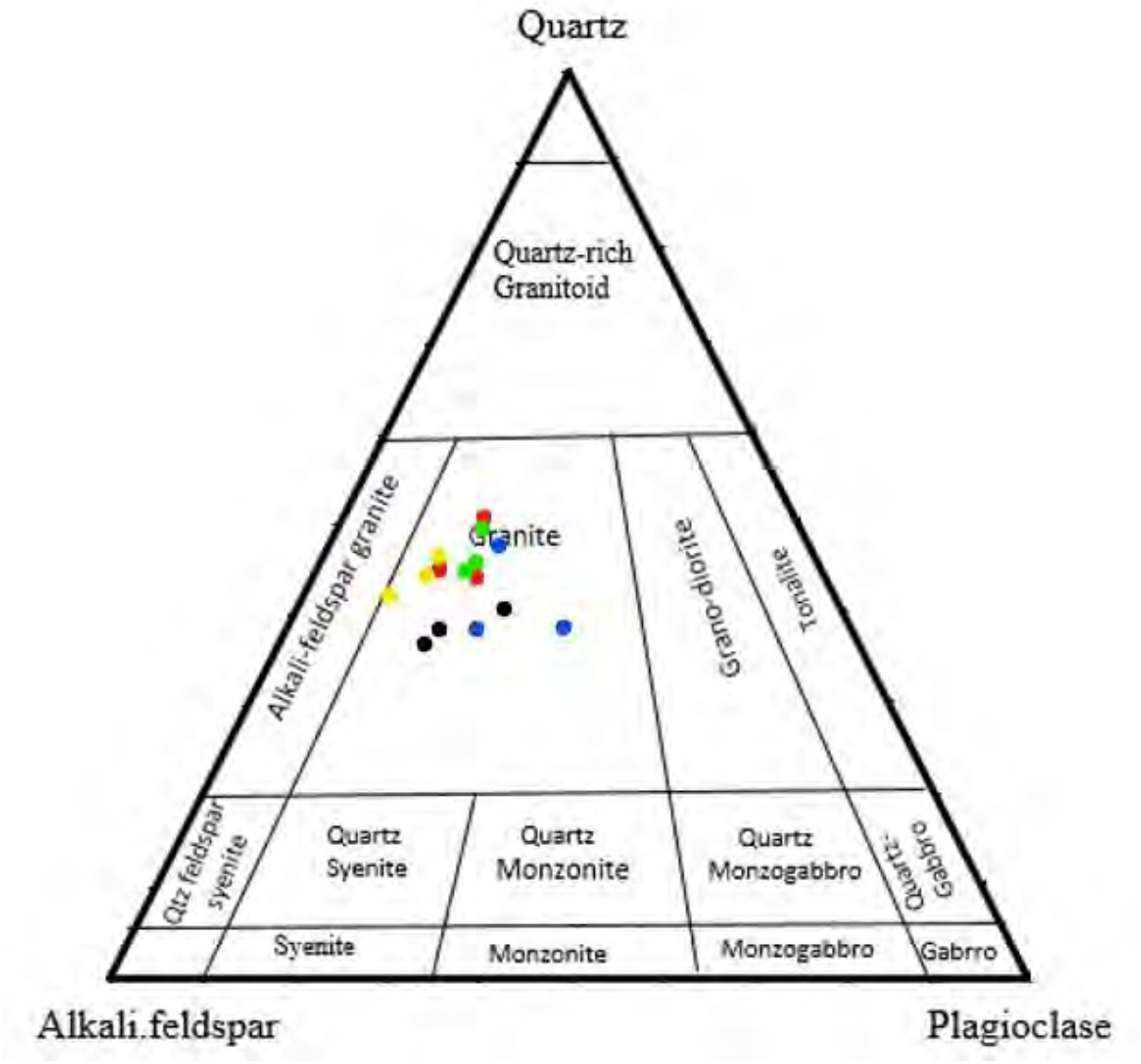


Fig. 4.27. Modal composition of the studied rocks plotted on the IUGS classification diagram (from Le Maitre, 2002).

Note: The black dots showing Shir Atraf coarse grained variety, the red dots showing Shir Atraf medium grained variety, the yellow dots showing Islampur coarse grained variety, the blue dots showing Islampur medium grained variety, and the green dots showing Islampur fine grained variety.

# CHAPTER 5 PHYSICAL AND MECHANICAL PROPERTIES

## 5.1. General Statement

In geological research, geologists recognise the naturally existing earth material known as rock, but civil engineers distinguish between rock and soil, although the distinction is not always clear. Engineers look for differences in the reaction or response of rock and soil to the force or load that they are subjected to, such as in construction. Rock mechanics is the study of the response of rocks to an applied pressure or force, whereas soil mechanics is the study of the response of soil to a force or load (Farmer., 1983). Rock can be described from a geological point of view, such as its origin, mineralogical content, and texture, or from an engineering point of view. The term texture in petrology refers to the size, shape, and distribution of minerals in a rock (McPhie et al., 1993; Bucher and Frey., 1994) It also reveals us about the rock's genesis and tectonic history (Akessan et al., 2003). The physical character of a rock is influenced by its texture, particularly the grain size. Fine-grained rocks are typically stronger than coarse-grained rocks (Bell., 2007). The rocks strength falls when alteration and weathering occur in it (Bell., 2007).

Various geological factors have a significant impact on the design, building, operation, and maintenance of engineering works. These factors include physical and mechanical properties of rocks. Mineral composition, alteration, grain shape, grain size, density, grain-size distribution, recrystallisation all have an impact on mechanical properties (Johnson and De Graff, 1988, Mc Phie et al., 1993; Raisanan., 2004; Bell, 2007 Undul and Tugrul, 2012; Zhang et al., 2012; Coggan et al., 2013; Sajid and Arif, 2015; Wazir et al., 2015). Because of their suitability some rocks are mostly used in several engineering projects. Microfractures, grain contact types, mineral twinning, and cleavage planes all have an impact on the rock's mechanical properties and strength and can operate as a zone of weakness (Willard and McWilliams., 1969). Rocks' intrinsic features, such as minerology and texture, can be used to assess their engineering properties (Lindqvist et al., 2007).

Several authors have investigated the relationship between petrographic characteristics and mechanical properties in northern Pakistan (Sajid and Arif, 2014, Arif et al., 1999; Din and Rafiq., 1997; Din et al., 1993). All these authors have worked on petrography and mechanical properties of granites in NW Pakistan, but the petrography and mechanical properties of Swat granitic gneisses has absented. the main theme of our study is to expose these properties of Swat granitic gnisses in two specific sections (Islampur and Shir Atraf areas).

## 5.2. Physical and mechanical properties

Physical and mechanical properties have following below:

- Strength Tests (UCS and UTS)
- Water absorption
- Specific gravity
- Porosity

### 5.2.1. Strength tests

The ability of a rock to resist the effect of applied stresses without large-scale failure is referred to as rock strength. Typically, the strength of a rock is determined experimentally through laboratory testing of fresh (undeform) samples. A rock's strength is determined by its constituent minerals; no rock can be stronger than the minerals it contains. In simple words, the nature of the minerals present in a rock has a great effect on the behaviour of the rock (Price and Freitas., 1995). The un-weathered sample can be tested in the laboratory, which is more accurate, cheaper, and simple to do, and reasonably more acceptable than field tests. However, rock characteristics can change within a small region, and a joint or fault system in the rock mass may affect the rock's behaviour in ways that cannot be determined through laboratory tests (Din et al., 1993). Paterson., 1978 determined that laboratory tests depend on the following factors:

- Rock type
- Rock composition
- Rock grain size
- Rock density and porosity
- Geometry, size, and shape of the test specimens
- Rate of loading
- Water pore pressure and saturation
- Testing apparatus (end effects, stiffness)
- Temperature
- Time

There are many tests for strength in laboratory (Unconfined compressive strength, Unconfined tensile strength, splitting tension test, Beam bending test, Ring shear test, etc) but we perform only UCS (Uniaxial compressive strength) and UTS (Uniaxial tensile strength).

### a. Uniaxial compressive strength

The load or stress per unit area at which a sample fails or breaks under compression is referred to as the UCS (Price and Freitas., 1995). Confining stress is zero, it is also known as a material's unconfined compressive strength (Price and Freitas., 1995). The UCS values are given in table 5.1.

**Procedure**

The test specimen for UCS tests must be right circular cylinders, according to ASTM-D2938. The core samples for UCS were taken from the bulk samples with core drilling machine, and its ends were cut (through rock cutting machine) and polished to distribute the load uniformly. The samples were inserted into the universal testing machine, which applied the load slowly and without shock. The load at the time of failure was noted and the uniaxial compressive strength was determined by the following formulas:

$$UCS = \frac{p}{A} (KN/m^2) \quad \text{.....eq(1)}$$

- P = Load at the time of failure (KN)
- A = Cross-sectional area of core ($m^2$) = $\frac{\pi D2}{4}$

OR

$$\sigma C = \frac{F}{A} (Lbf / inch^2) \quad \text{.....eq(2)}$$

- $\sigma C$ = unconfined compressive strength
- A = cross section area of core sample $(inch)^2$.
- F = maximum Failure Load (Lbf)

Both the eq(1) and eq(2) is used to determining the UCS test value but unit is different in these equations.

Table. 5.1. Showing UTS values.

| Uniaxial Compressive Strength (UCS) | | | | |
|---|---|---|---|---|
| **Sample No.** | **Area (inch)$^2$** | **load (lbf)** | **Strength (psi)** | **Strength (Mpa)** |
| **SGC1** | 5.8 | 50305 | 8673 | 59.79 |
| **SGC2** | 5.8 | 51480 | 8876 | 61.2 |
| **SGC3** | 5.8 | 51850 | 8939 | 61.63 |
| **SGM1** | 5.8 | 52856 | 9113 | 62.83 |
| **SGM2** | 5.8 | 54652 | 9422 | 64.96 |
| **SGM3** | 5.8 | 51458 | 8872 | 61.17 |
| **IGC1** | 5.8 | 50089 | 8663 | 59.54 |
| **IGC2** | 5.8 | 46682 | 8049 | 55.48 |
| **IGC3** | 5.8 | 50703 | 8742 | 60.27 |
| **IGM1** | 5.8 | 54317 | 9365 | 64.56 |
| **IGM2** | 5.8 | 53515 | 9227 | 63.61 |
| **IGM3** | 5.8 | 52427 | 9039 | 62.32 |
| **IGF1** | 5.8 | 69401 | 11965 | 82.5 |
| **IGF2** | 5.8 | 66574 | 11478 | 79.13 |
| **IGF3** | 5.8 | 62307 | 10742 | 74 |

**b. Uniaxial tensile strength (UTS)**

To test the tensile strength of a rock sample, a uniaxial tensile force is applied to a rock sample. The tensile strength of a material is 8 to 10 times that of compressive strength. It means UTS is always greater than UTS (Tariq and Majid., 1998; Bell., 2007). This test determines the tensile strength of a sample by creating tension across its diameter while it is compressed by a vertical force. From the cores, disc form samples with a thickness to diameter ratio of were chosen, as required by UTS. Following that, the samples were put into the universal testing machine, and the load at the time of failure was recorded. The UTS values are given in table 5.2. The UTS was then determined by the following formula:

$$UTS = \frac{2P}{\pi DT} \quad \ldots\ldots\ldots\ldots\ldots\ldots\ldots\ldots\ldots\ldots\ldots\ldots\ldots\ldots\ldots\ldots eq(1)$$

- P = Load at failure (KN)
- D = Diameter of the rock core (m)
- T = Thickness of the rock core (M)

OR

$$\sigma T = \frac{F}{A} (Lbf / inch^2) \ldots\ldots\ldots\ldots\ldots\ldots\ldots\ldots\ldots\ldots eq(2)$$

- $\sigma T$ = unconfined compressive strength
- A = cross section area of core sample (inch) $^2$.
- F = maximum Failure Load (Lbf)

Both the eq(1) and eq(2) is used to determining the UTS test value but unit is different in these equations.

Table. 5.2. Showing UTS values.

| **Uniaxial Tensile Strength (UTS)** | | | | |
|---|---|---|---|---|
| **Sample No.** | **Area(inch)$^2$** | **Load(lbf)** | **Strength (Psi)** | **Strength (Mpa)** |
| **SGC1** | 4.1 | 3884 | 947 | 6.5 |
| **SGC2** | 4.4 | 5029 | 1142 | 7.8 |
| **SGC3** | 4.4 | 4996 | 1135 | 7.8 |
| **SGM1** | 4.4 | 3329 | 757 | 5.2 |
| **SGM2** | 4.1 | 4632 | 1129 | 7.7 |
| **SGM3** | 4.1 | 2234 | 545 | 3.8 |
| **IGC1** | 4.4 | 2909 | 661 | 4.5 |
| **IGC2** | 4.1 | 2493 | 609 | 4.2 |
| **IGC3** | 4.1 | 2940 | 717 | 4.9 |
| **IGM1** | 4.4 | 2855 | 649 | 4.5 |
| **IGM2** | 4.4 | 2409 | 547 | 3.7 |
| **IGM3** | 4.1 | 2147 | 524 | 3.6 |
| **IGF1** | 4.1 | 2632 | 642 | 4.4 |
| **IGF2** | 4.1 | 2429 | 592 | 4.0 |
| **IGF3** | 4.1 | 2341 | 571 | 3.9 |

### 5.2.2. Specific gravity:

The proportion of the weight of a particular volume of material to an equal volume of water is known as specific gravity. specific gravity, also called relative density, ratio of the density of a substance to that of a standard substance (water). For heavy construction activity, a specific gravity greater than 2.55 is regarded to be suitable (Blyth and deFreitas., 1974). The specific values of the samples given in table 5.3.

To determine the specific gravity of the given rock samples the equipment's will be used which are beaker, digital balance, thread, and water. Sample were obtained and weighted in air, with the results recorded as dry weight(W1), and then the sample were plunged in water and weighted under suspended conditions, with the results recorded as weight in water(W2). The following formula was used to calculate the specific gravity results:

$$SG = \frac{W1}{W1-W2}$$

- SG = Specific Gravity
- W1 = Weight of sample in air
- W2 = Weight of sample immersed in water

### 5.2.3. Porosity

The porosity of a rock indicates how densely it is packed. The ratio of the volume of pores to the volume of bulk rock is known as porosity, and it is commonly stated as a percentage. Different factors affect the porosity of rock for example grain size (fine, medium, or coarse grain), grain shape, mineralogical composition, etc. For example, fine grain rock has low porosity as compared to coarse grain rock. The porosity of the samples given in table 5.3. The porosity of the samples studied was determined using the saturation method, and the formula below was used to calculate it.

$$\Phi = \frac{Wa-Wd}{Wa-Ww} \times 100$$

Note; Φ = Porosity, Wa = Weight in air, Wd = Dry weight and Ww = Weight in water

### 5.2.4. Water absorption

Water absorption is the process of water entering and degrading the pore spaces of rocks. Water penetration is a critical factor in evaluating the durability of rocks for use as construction materials (Shakoor and Bonelli., 1991). Simply water absorption refers to how quickly a rock can absorb water and is evaluated with a water absorption test. In 1982, the American Society

for Testing and Materials (ASTM) recommended evaluating at least three samples for water absorption. The water absorption values of the samples given in table 5.3. To determine water absorption, samples were first dried in an oven at temperatures ranging from 105 to 110 C°. Then it was cooled and weighed as (W1). After that, the same sample was kept in distilled water for 24 hours before being weighed again (W2). Water absorption was calculated using the formula below.

$$WA = \frac{W2-W1}{W2}$$

- WA = Water Absorption
- W1 = Dry weight
- W2 = Wet weight

Table. 5.3. Showing specific gravity, porosity, and water absorption values.

| Samples | Wt in Air (grams) | Wt in Water (grams) | Oven Dry Wt (grams) | Water Absorption | % Water Absorption | Specific Gravity | Porosity in % |
|---|---|---|---|---|---|---|---|
| **SGC1** | 1371.90 | 855.37 | 1370.94 | 0.96 | 0.07 | 2.658 | 0.19 |
| **SGC2** | 1359.97 | 848.03 | 1359.03 | 0.94 | 0.07 | 2.659 | 0.18 |
| **SGC3** | 1362.24 | 850.58 | 1361.49 | 0.75 | 0.06 | 2.664 | 0.15 |
| **SGM1** | 1361.1 | 851.49 | 1360.37 | 0.73 | 0.05 | 2.672 | 0.14 |
| **SGM2** | 1359.14 | 848.58 | 1358.48 | 0.66 | 0.05 | 2.663 | 0.13 |
| **SGM3** | 1392.02 | 869.18 | 1391.06 | 0.96 | 0.07 | 2.664 | 0.18 |
| **IGC1** | 1298.4 | 813.46 | 1298.04 | 0.36 | 0.027 | 2.677 | 0.074 |
| **IGC2** | 1327.85 | 831.81 | 1327.46 | 0.39 | 0.028 | 2.676 | 0.08 |
| **IGC3** | 1293.72 | 811.22 | 1293.4 | 0.32 | 0.024 | 2.681 | 0.065 |
| **IGM1** | 1314.8 | 821.8 | 1314.47 | 0.33 | 0.025 | 2.666 | 0.066 |
| **IGM2** | 1323.13 | 826.05 | 1322.78 | 0.35 | 0.026 | 2.676 | 0.07 |
| **IGM3** | 1317.36 | 827.02 | 1316.97 | 0.39 | 0.029 | 2.686 | 0.08 |
| **IGF1** | 1364.37 | 845.87 | 1363.98 | 0.39 | 0.029 | 2.661 | 0.075 |
| **IGF2** | 1311.16 | 815.16 | 1310.71 | 0.45 | 0.033 | 2.643 | 0.09 |
| **IGF3** | 1348.21 | 847.25 | 1347.73 | 0.48 | 0.035 | 2.691 | 0.1 |

Table. 5.4. Showing all combine value of UCS, UTS, specific gravity, porosity, and water absorption values.

| Samples | UCS (Mpa) | UTS (Mpa) | % Water Absorption | Specific Gravity | Porosity in % |
|---|---|---|---|---|---|
| **SGC1** | 59.79 | 6.5 | 0.06 | 2.664 | 0.15 |
| **SGC2** | 61.2 | 7.8 | 0.07 | 2.659 | 0.18 |
| **SGC3** | 61.63 | 7.8 | 0.07 | 2.658 | 0.19 |
| **SGM1** | 62.83 | 5.2 | 0.07 | 2.664 | 0.18 |
| **SGM2** | 64.96 | 7.7 | 0.05 | 2.663 | 0.13 |
| **SGM3** | 61.17 | 3.8 | 0.05 | 2.672 | 0.14 |
| **IGC1** | 59.54 | 4.5 | 0.028 | 2.676 | 0.078 |
| **IGC2** | 55.48 | 4.2 | 0.027 | 2.677 | 0.074 |
| **IGC3** | 55.48 | 4.9 | 0.024 | 2.681 | 0.065 |
| **IGM1** | 64.56 | 4.5 | 0.025 | 2.666 | 0.066 |
| **IGM2** | 63.61 | 3.7 | 0.026 | 2.676 | 0.07 |
| **IGM3** | 62.32 | 3.6 | 0.029 | 2.686 | 0.08 |
| **IGF1** | 82.5 | 4.4 | 0.029 | 2.661 | 0.075 |
| **IGF2** | 79.13 | 4.0 | 0.033 | 2.643 | 0.09 |
| **IGF3** | 74 | 3.9 | 0.035 | 2.691 | 0.1 |

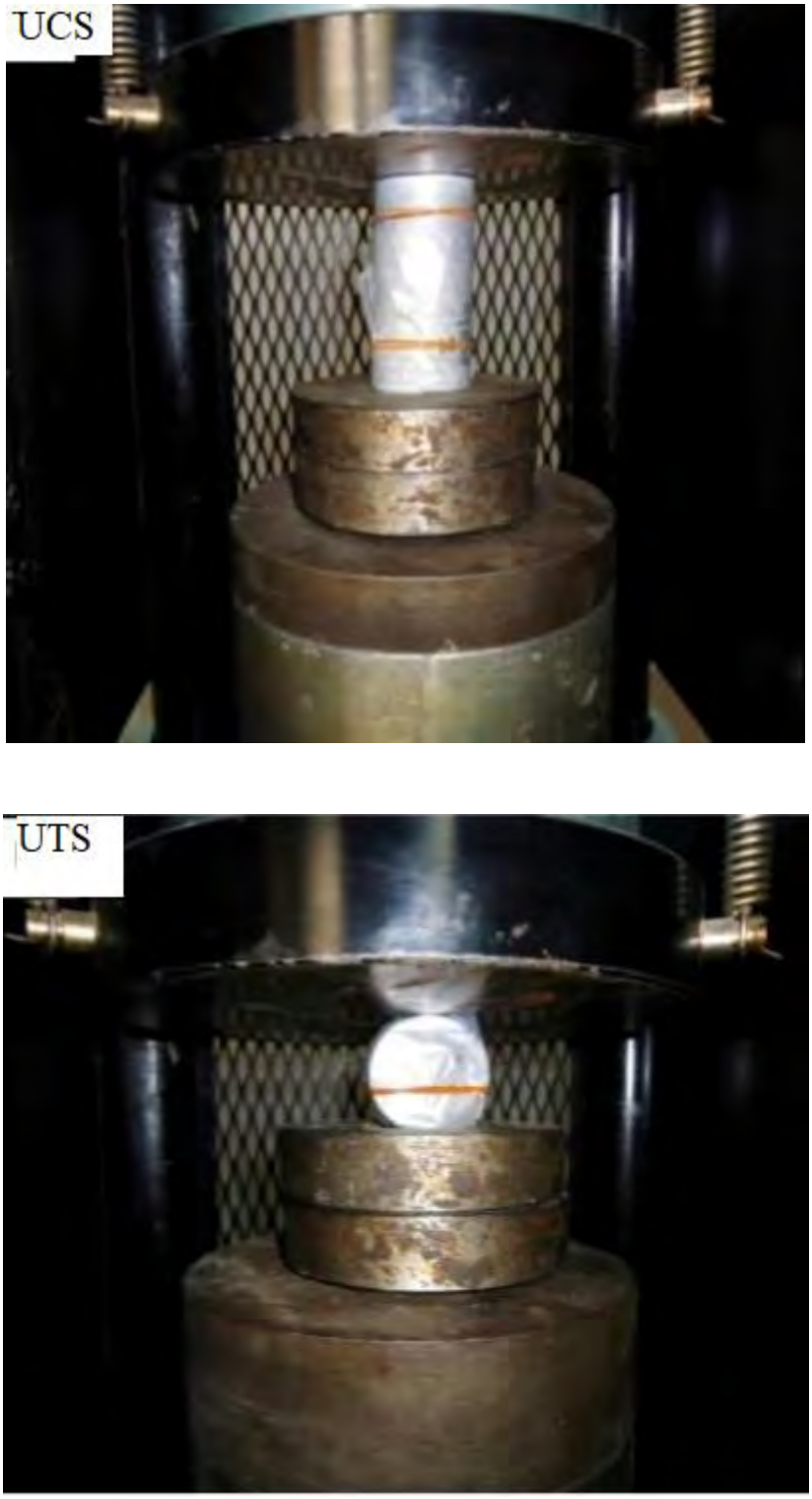


Fig. 5.1. Universal testing machine (UTM), sample for UCS test and Universal testing machine (UTM), sample for UTS test


Fig. 5.2. Rock cutting machine

# CHAPTER 6 RELATIONSHIP AMONG PETROGRAPHIC, PHYSICAL AND MECHANICAL PROPERTIES

## 6.1. General Statement

The petrographic, physical, and mechanical properties of the different textural varieties of Swat granitic gneisses are plotted against each other to investigate if there is a possible relationship between them.

Mineral composition, alteration, grain shape, grain size, density, grain-size distribution, micro-fractures, grain contact types, degree of weathering, cleavage planes, recrystallisation all have an impact on mechanical properties (Willard and McWilliams, 1969; Johnson and De Graff., 1988; Mc Phie et al., 1993; Hecht et al., 2005; Raisanan., 2004; Bell, 2007; Lindqvist et al., 2007). Some of these features have direct relation while some have inverse relation with physical and mechanical properties.

Individual mineral concentration and composition are important considerations when analysing the overall strength of a rock (Tugrul., 2004; Lindqvist et al., 2007; Yilmaz et al., 2011). When comparing the behaviour of quartz and calcite when interacting with acidic hydrothermal fluids, the mineral composition is likely to be very sensitive to certain types of alteration. Although silicate minerals are generally more resistant to chemical weathering than carbonate minerals, some silicate minerals, such as nepheline, weaken significantly when exposed to acidic fluids (Lindqvist et al., 2007). Irfan and Dearman (1978), Irfan (1996), and Mendes et al., (1966) proposed indices based on the percentage of sound and unsound minerals. The higher value of the index indicates less weathering and mechanically sound nature of the rock.

$$Ip = \text{sound constituents \%} / \text{unsound constituents \%}$$

Ip = index indicates, sound constituents = primary rock forming minerals, unsound constituents = alteration products of major rock forming minerals i.e., kaolinite after feldspar or serpentine after olivine.

Onodera et al., (1974) used a point counting method to describe an index based on the density of micro fractures along the length of a measured traverse. Higher fracture density was linked to a mechanically weaker rock.

## 6.2. UCS VS Q/F Ratio

Quartz to feldspar ratios have a direct correlation, as shown by the graphs (Fig. 6.1). A similar relationship is noted by Tugrul and Zarif (1999) and Gunsallus and Kulhawy (1999).

**Note:** All the plots of this chapter have different shapes for the rock varieties i.e., in Shir Atraf granitic gneisses the black plus represent coarse grained variety, the red circles represent medium grained variety. In Islampur granitic gneisses the squares represent coarse grained variety, the blue triangles represent medium grained variety, and the green crosses represent fine grained variety.

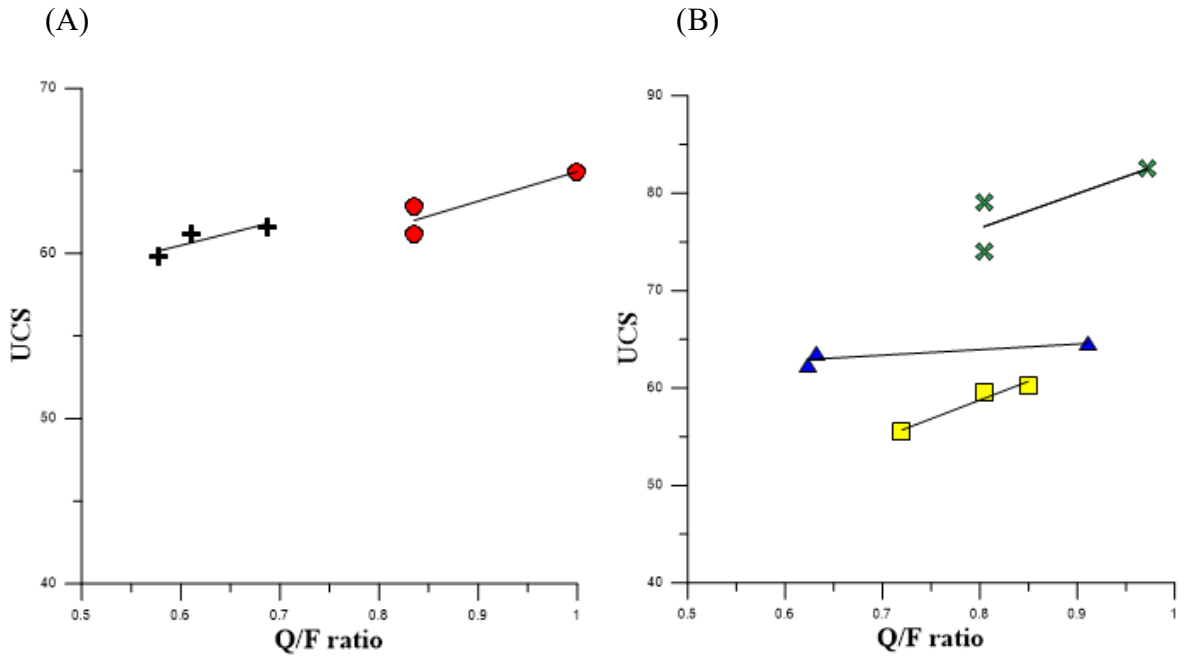


Fig. 6.1. Relationship between UCS and Q/F ratio: (A) Shir Atraf granitic gneisses (B) Islampur granitic gneisses.

## 6.3. UCS VS Quartz

The concentration of quartz correlates positively with the strength of granitic rocks from various regions (Tugrul and Zarif., 1999; Khalil et al., 2015; Sajid and Arif., 2015). however, similar comparisons can describe a negative relation. (Sousa et al., 2013) or no relation (Yilmaz et al., 2011) with granites from other areas. Current work shows a positive impact of quartz on UCS (Fig. 6.2). The strength values increase with increase in quartz concentration.

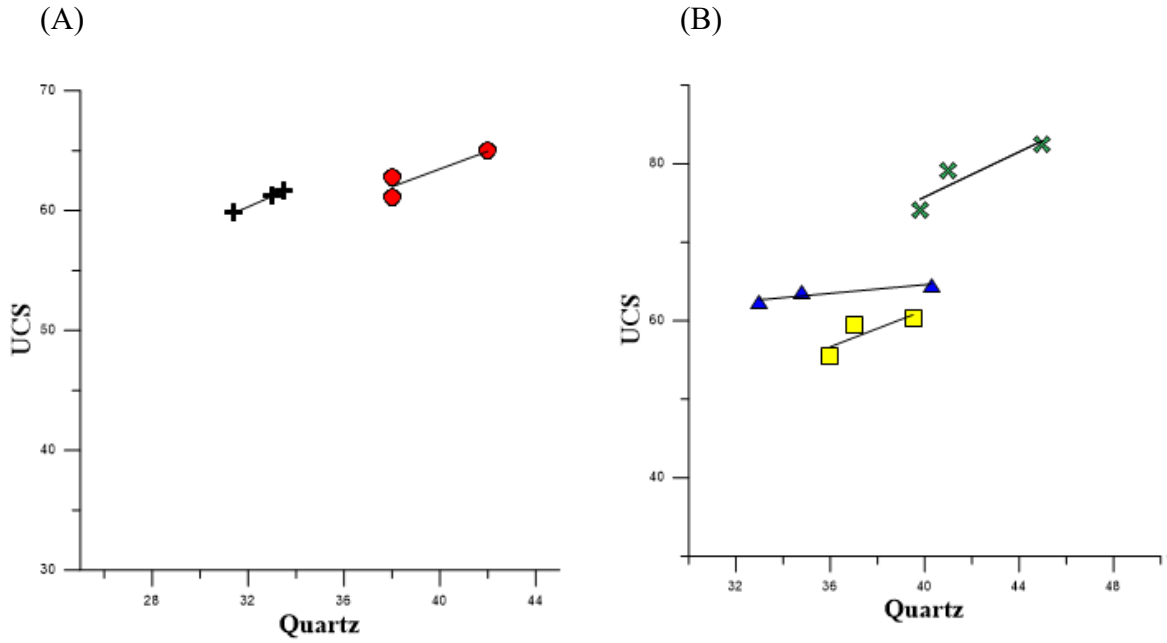


Fig. 6.2. Relationship between UCS and Quartz: (A) Shir Atraf granitic gneisses (B) Islampur granitic gneisses.

## 6.4. UCS VS Porosity

The UCS values of the studied samples are plotted against their porosity values. The resulting plots shows a negative correlation between porosity and UCS (Fig. 6.3). Increase in the porosity in a rock obviously decreases its strength (Tugrul and Zarif., 1999).

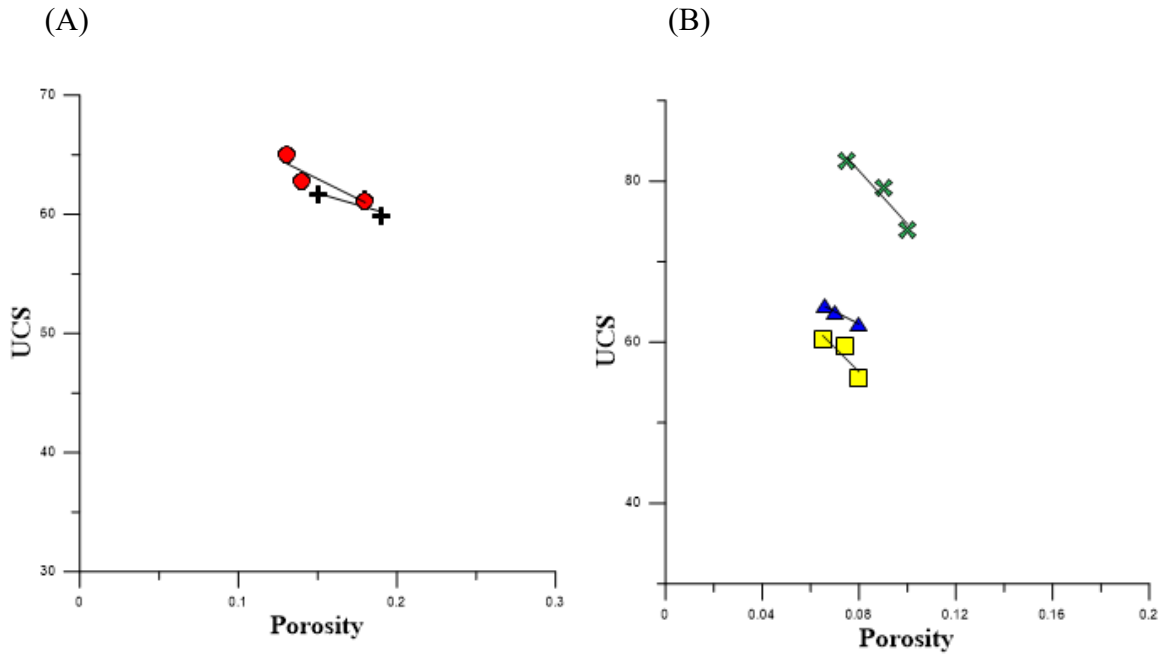


Fig. 6.3. Relationship between UCS and porosity: (A) Shir Atraf granitic gneisses (B) Islampur granitic gneisses.

## 6.5. UTS VS Q/F Ratio

To see the relationship between quartz to felspar ratio and UTS, have a direct correlation, as shown by the graphs (Fig. 6.4). It means that if the quartz to felspar ratio increase the value of UTS increase. A similar relationship is noted by Tugrul and Zarif (1999) and Gunsallus and Kulhawy (1999).

(A) (B)

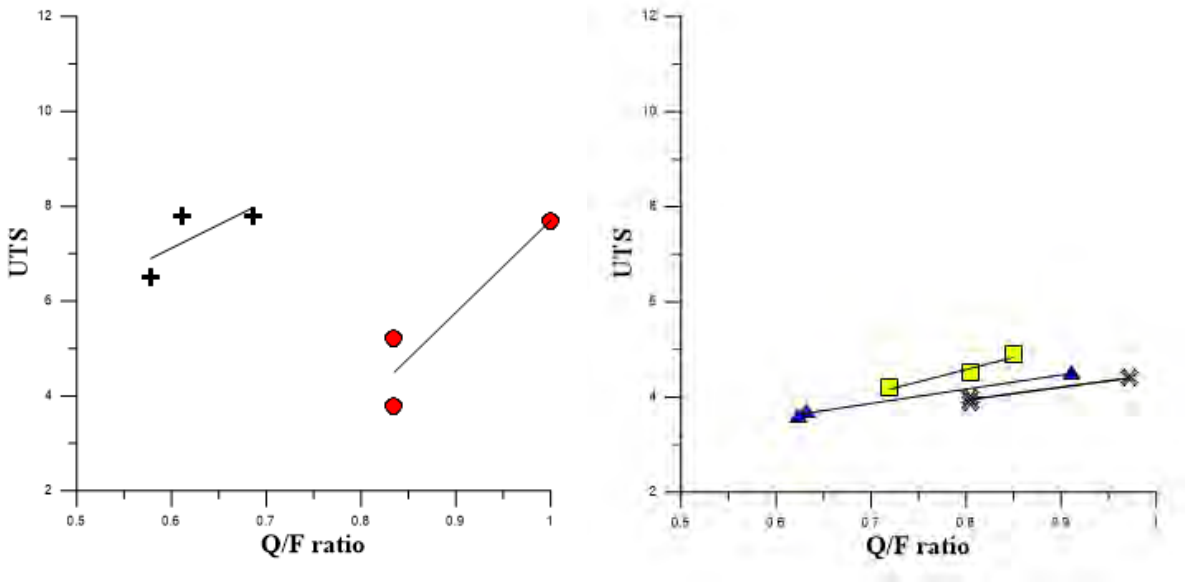


Fig. 6.4. Relationship between UTS and Q/F ratio: (A) Shir Atraf granitic gneisses (B) Islampur granitic gneisses.

## 6.6. UCS VS Water Absorption

UCS values of the investigated samples are plotted against their porosity and water absorption values (Fig. 6.5) which show inverse relation.

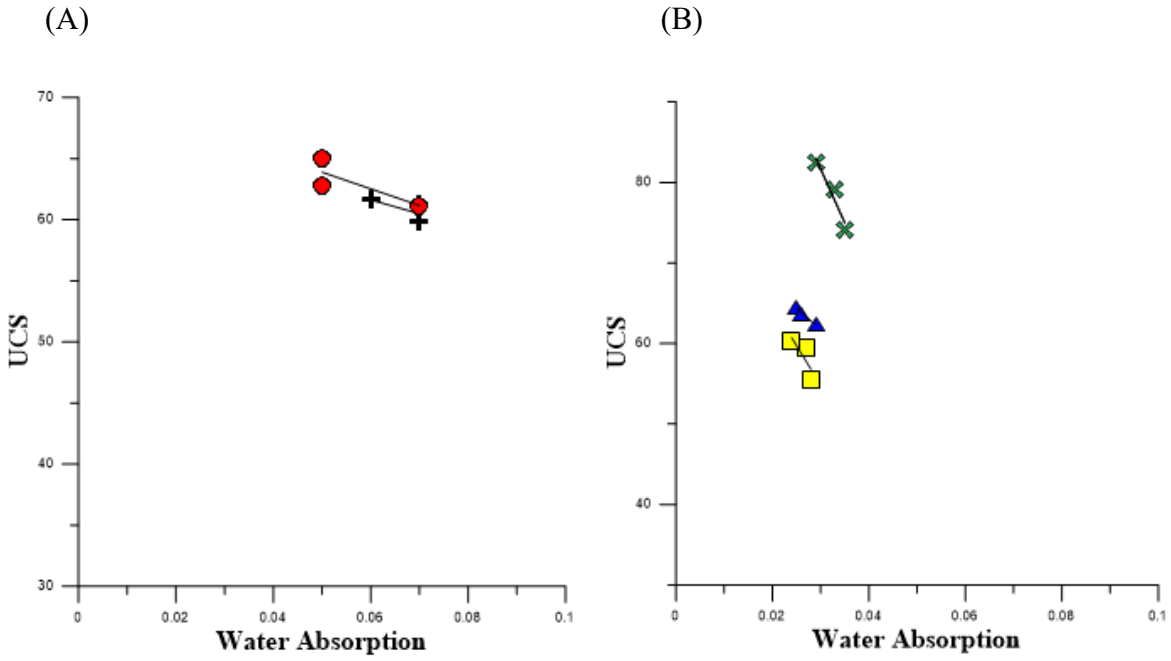


Fig. 6.5. Relationship between UCS and water absorption: (A) Shir Atraf granitic gneisses (B) Islampur granitic gneisses.

## 6.7. UCS VS Mica

The mica content is plotted against the UCS values of the samples under investigation. In Shir Atraf granitic gneisses the plot between the mica and UCS show inverse relation (Fig. 6.6). In Islampur granitic gneisses only the fine-grained variety show inverse relation and other two varieties (medium-grained and coarse-grained) have no significant relation is interpreted from these plots.

(A)

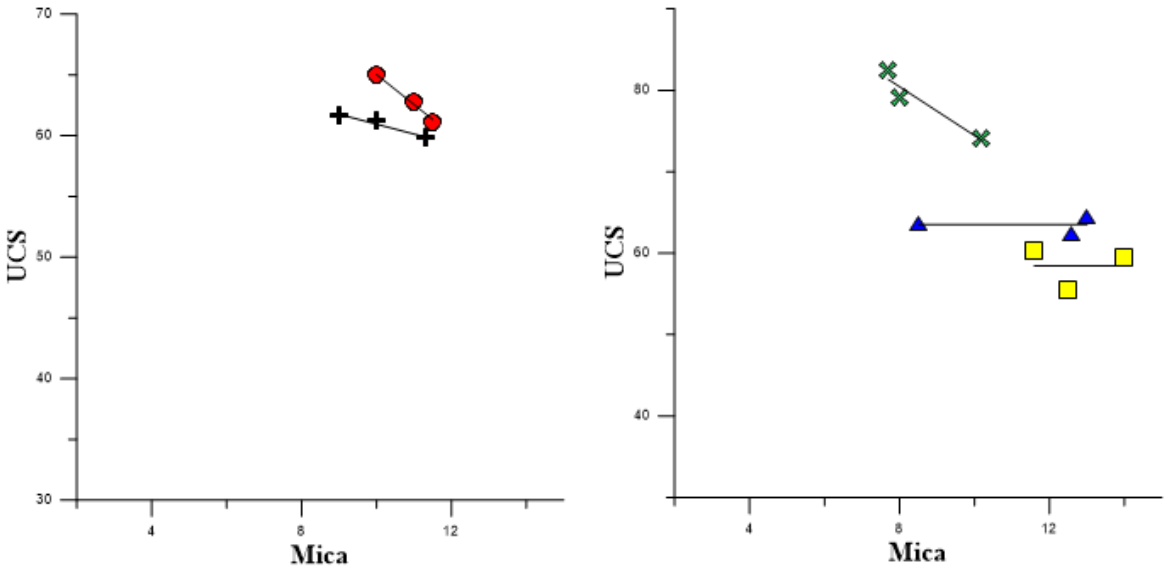


Fig. 6.6. Relationship between UCS and Mica content: (A) Shir Atraf granitic gneisses (B) Islampur granitic gneisses.

## 6.8. UCS VS UTS

The UCS versus UTS plots shows a direct relation (Fig. 6.7). The USC-UTS plot was used by Tugrul and Gurpinar (1997), Shakoor and Bonelli (1991), and D'Andrea et al., (1965) and find a similar relationship for different rock types and found the same result.

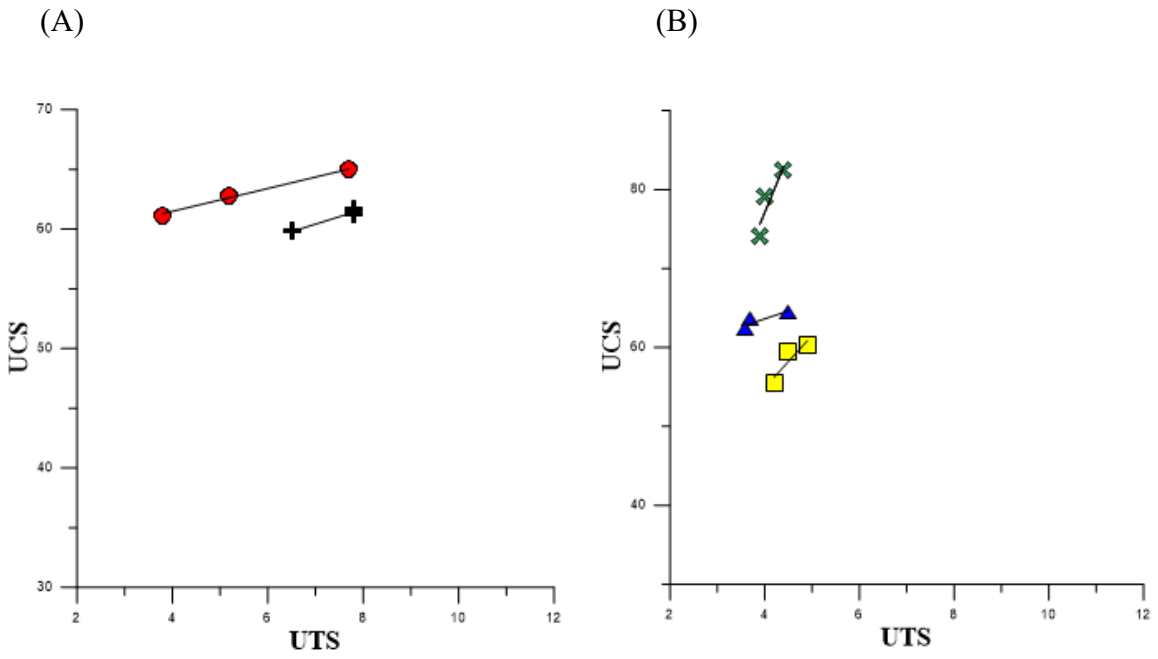


Fig. 6.7. Relationship between UCS and UTS: (A) Shir Atraf granitic gneisses (B) Islampur granitic gneisses.

## 6.9. Q/F Ratio VS Porosity

The quartz to feldspar ratios of the studied samples is plotted against their porosity values. The resulting plots shows negative correlation between porosity and quartz to feldspar ratio (Fig. 6.8).

(A)

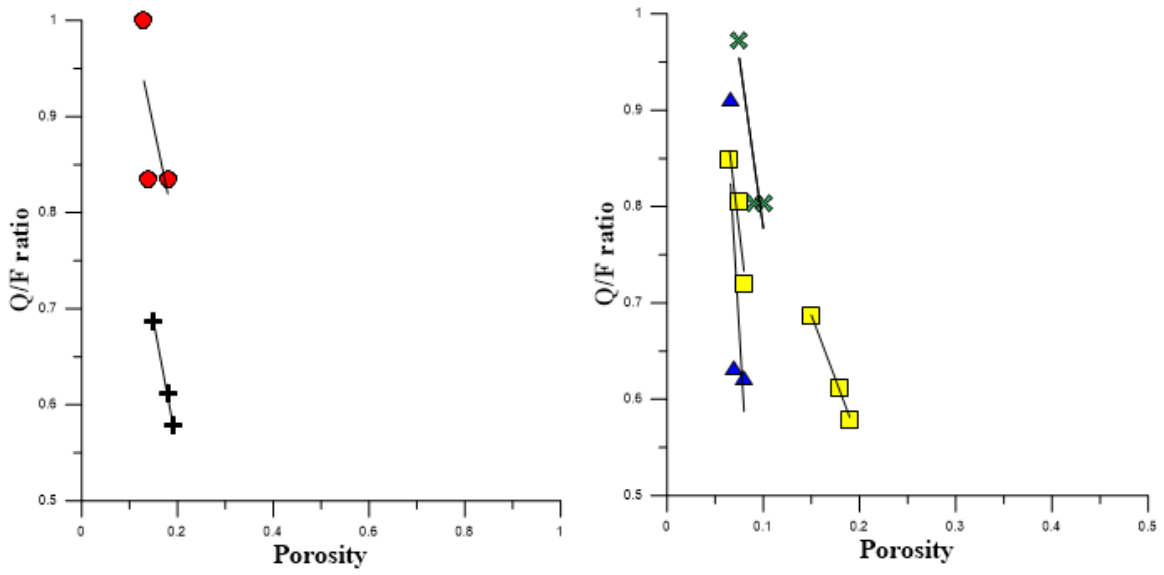


Fig. 6.8. Relationship between porosity and Q/F ratio: (A) Shir Atraf granitic gneisses (B) Islampur granitic gneisses.

## 6.10. Quartz VS Porosity

The total porosity of a rock is affected by its quartz content because anhedral quartz grains fill spaces between other grains (Tugrul and Zarif., 1999). Similar case repeated in the current study. The quartz content of the samples studied are plotted against their porosity values. The resulting plots shows negative correlation between porosity and quartz content (Fig. 6.9).

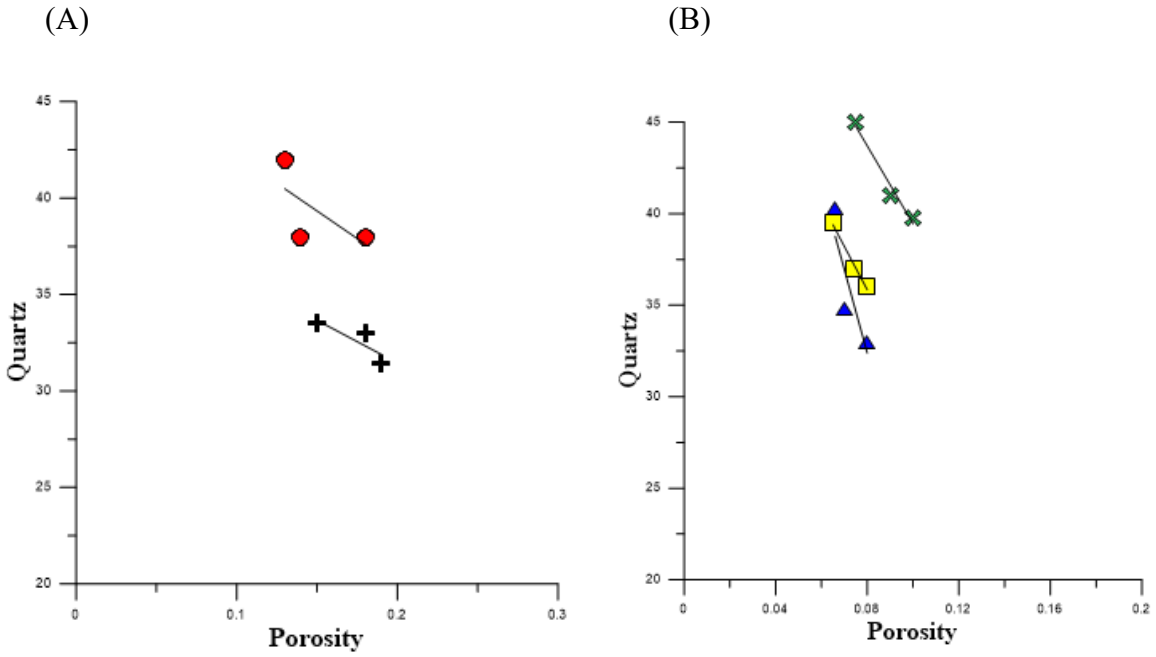


Fig. 6.9. Relationship between Quartz and porosity: (A) Shir Atraf granitic gneisses (B) Islampur granitic gneisses.

# CHAPTER 7 DISCUSSION AND CONCLUSION

## 6.1. General statement

The main objectives of this research are petrographic and physico-mechanical studies of granitic gneisses from the Shir Atraf and Islampur areas of Swat. The previous chapters provide information on the various methods used and the results obtained from these studies.

## 6.2. Petrography

Petrographically, the Swat granitic gneisses of Swat and Buner areas can be grouped into two i.e., the flaser granitic gneisses (light-colored, coarse-grained ground mass) and the Augen granodiorite gneisses (dark-colored, fine-grained ground mass) (DiPietro, 1990). In this research petrographically the Swat granitic gneisses have grouped into two Shir Atraf granitic gneisses (coarse and medium grained) and Islampur granitic gneisses (coarse, medium, and fine grained).

In Shir Atraf area Swat granitic gneisses contain quartz, alkali feldspar (orthoclase + microcline), plagioclase, biotite, muscovite, garnet, tourmaline, and ore minerals. Quartz, alkali feldspar and plagioclase constitute the groundmass with minor to accessory amounts of muscovite, and biotite and accessory to trace amounts of tourmaline (only brown tourmaline), garnet, epidote, chlorite, and ore minerals.

In Islampur area Swat granitic gneisses also contain quartz, alkali feldspar (orthoclase + microcline), plagioclase, biotite, muscovite, garnet, tourmaline, and ore minerals. Quartz and alkali feldspar constitute the groundmass with minor to accessory amounts of muscovite, and biotite and accessory to trace amounts of tourmaline (only brown tourmaline), garnet, epidote, chlorite, and ore minerals. Only the medium grain verity of Islampur contain very less amount of garnet and tourmaline. The fine gain variety of Islampur have no tourmaline, garnet, epidote, and chlorite in the present study. As compared to Shir Atraf area Islampur area has more quartz.

DiPietro (1990) reported the same minerals. Lawangin Sheikh (2020) also reported the same minerals and apatite, clinopyroxenes, and rutile from Swat granitic gneisses. No apatite, clinopyroxenes, and rutile (titanium dioxide) were found during this study, and none described by previous workers (DiPietro, 1990; Jan and Tahirkheli, 1969; King, 1964; Martin et al., 1962).

Rocks with a high concentration of physically strong minerals are obviously strong, but the textural relationship between these minerals and their associated minerals can also influence strength.

## 6.3. Mechanical properties

Some of the physical and mechanical properties of different textural varieties of Swat granitic gnisses were determined as part of the current study to assess their suitability for use as construction material. As described in chapter five, the strength values are shown in (Table 5.1). The UCS of all the samples (from both areas) falls within the range of those rocks designated as strong (Table 6.1).

This study attempts to establish a possible relationship between the petrographic characteristics, physical properties, and strength of these rocks. The rock samples' strength values are plotted against their physical properties and petrographic characteristics. According to a detailed comparison and thorough examination, the following petrographic features are the most important in determining and controlling the strength of the studied rocks.

- Modal mineralogical composition
- Grains size and shape
- Alignment mineral grains
- Volume of voids

The mean values of the investigated physical and mechanical properties of different textural varieties of Swat granitic gneisses are determined using statistical analysis (table 6.2). Fine-grained rocks are mostly found to be stronger than coarse-grained rocks (Bell., 2007). However, a comparison of the current investigation's results yields the exact same conclusion. The Shir Atraf medium grained variety has found to be stronger than coarse-grained variety. Similarly, in Islampur area the fine-grained variety has stronger than medium and coarse-grained variety.

Table 7.1. Grades of unconfined compressive strength.

| Geological Society (Anon, 1977) | | IAEG* (Anon, 1979) | | ISRM** (Anon, 1981) | |
|---|---|---|---|---|---|
| **Description** | **UCS (MPa)** | **Description** | **UCS (MPa)** | **Description** | **UCS (MPa)** |
| Very weak | <1.25 | Weak | <15 | Very low | <6 |
| Weak | 1.25-5.00 | Moderately weak | 15-50 | Low | 6-10 |
| Moderately weak | 5.00-15.50 | Strong | 50-120 | Moderate | 20-60 |
| Moderately strong | 12.50-50 | Very strong | 120-130 | High | 60-200 |
| Strong | 50-100 | Extremely Strong | Over 230 | Very high | Over 200 |
| Very strong | 100-200 | | | | |
| Extremely Strong | Over 200 | | | | |

*International Association of Engineering Geologists
**International Society for Rock Mechanics

Table 7.2. Average values of UCS, UTS, porosity, water absorption, specific gravity, quartz to feldspar ratio and mica content of the studied samples.

| S. No | UCS | UTS | Porosity | WA | SG | Q/F r | Quartz | Mica |
|---|---|---|---|---|---|---|---|---|
| **SGC** | 60.8 | 7.3 | 0.17 | 0.06 | 2.66 | 0.62 | 33.3 | 10.1 |
| **SGM** | 63 | 5.6 | 0.15 | 0.05 | 2.666 | 0.89 | 39.3 | 10.8 |
| **IGC** | 58.4 | 4.5 | 0.07 | 0.02 | 2.678 | 0.7 | 37.5 | 12.7 |
| **IGM** | 63.2 | 4 | 0.07 | 0.02 | 2.676 | 0.72 | 37 | 11.3 |
| **IGF** | 78.5 | 4.1 | 0.08 | 0.03 | 2.665 | 0.85 | 42 | 8.6 |

## 6.4. Conclusions

In the previous chapters, various details about field and petrographic observations, as well as mechanical properties of granitic gneisses from the Swat area, were presented. As a result of these discussions, the following conclusions were obtained:

1. According to the sample collection areas, the Swat granitic gneisses of the Swat area are divided into two categories in the current work.
    a. Shir Atraf granitic gneisses. This area contains two different varieties i.e., coarse-grained, and medium grained.
    b. Islampur granitic gneisses. This area contains three different varieties i.e., coarse-grained, medium grained and fine grained.
2. Petrographically these rocks are inequigranular, porphyritic and allotriomorphic in nature. Thin sections observation under a microscope reveals a variety of minerals, including quartz, plagioclase, and alkali feldspar, which are abundant. Biotite, muscovite, epidote, chlorite, garnet, tourmaline, and ore minerals are also present in minor to accessory amount.
3. Plagioclase present as a phenocryst, while quartz and alkali feldspar mostly occupy the ground mass. Biotite and muscovite are subhedral to anhedral in form and no clear layering has present. Some biotite grains have altered to epidote and chlorite. Fractured garnet has also present. Brown tourmaline grains are also present in discrete form. Some ore grains are embedded in other minerals.
4. A combination of petrographic features, including mineralogical composition, grain size and shape distribution, modal abundance and orientation of flaky minerals, and the volume of empty spaces, appears to have determined the actual strength of the Swat granitic gneisses.
5. The concentration of quartz shows positive impact on strength values. The Q/F ratios have also direct relation with strength.
6. The mica concentration shows negative impact on strength values. In two varieties (Islampur coarse and fine grained) mica have shown no relation with strength.
7. Porosity and water absorption show the negative impact on strength of rock. All the plot of porosity and water absorption with UCS values clearly show this negative impact.

8. The UCS values lie between 50 to 100 Mpa. According to the Geological Society (Anon., 1977) these values lie in the category of moderately strong, and are feasible for construction materials such as foundations, road constructions and buildings.

# REFRENCES


- Ahmad, Irshad, Joseph A. Dipietro, Kevin R. Pogue, Robert D. Lawrence, Mirza S. Baig, and Ahmad Hussain. "Stratigraphy south of the Main Mantle Thrust, Lower Swat." (1993)
- Ahmed, Z., & Chaudhry, M. N. (1976). Petrology of the Babusar area, Diamir district, Gilgit, Pakistan. *Geological Bulletin, Punjab University*, *12*, 67-78.
- Anjum, M. N., Arif, M., & Ali, L. (2018). Mineralogical and beneficiation studies of the Fe Cu ores of Dammal Nisar, Chitral, NW Himalayas Pakistan. *Journal of Himalayan Earth Sciences*, *51*(2A), 108-119.
- ARIF, M., RAHMANULLAH, I. A., & KHAN, K. (2002). PETROGRAPHY OF THE URANIFEROUS QUARTZOFELDSPATHIC VEINS AND THEIR WALL ROCK FROM MARGHAZAR, LOWERSWAT, PAKISTAN. *The Geological Bulletin of the Panjab University*, (37), 57.
- Armbruster, J., Seeber, L., & Jacob, K. H. (1978). The northwestern termination of the Himalayan Mountain front: active tectonics from microearthquakes. *Journal of Geophysical Research: Solid Earth*, *83*(B1), 269-282.
- Baud, A. Y. M. O. N., Gaetani, M., Garzanti, E., Fois, E., Nicora, W., & Tintori, A. (1984). Geological oservation in southeastern Zanskar and adjacent Lahul area (northern Himalaya). *Eclogae Geologicae Helvetiae*, *77*(1), 177-197.
- Bell, F. G. (1978). Petrographical factors relating to porosity and permeability in the Fell Sandstone. *Quarterly Journal of Engineering Geology and Hydrogeology*, *11*(2), 113 26.
- Bell, F. G. (2007). *Basic environmental and engineering geology* (No. 631.47 B433). Whittles Publishing.
- Blyth, F. G. H., & De Freitas, M. H. (2017). *A geology for engineers*. CRC Press.
- Blyth, F.G.H., DeFreitas, M.H., 1974. A geology of engineers. ELBS and Edward Arnold, London.
- Brookfield, M. E. (1993). The Himalayan passive margin from Precambrian to Cretaceous times. *Sedimentary Geology*, *84*(1-4), 1-35.
- Brozović, N., Burbank, D. W., & Meigs, A. J. (1997). Climatic limits on landscape development in the northwestern Himalaya. *Science*, *276*(5312), 571-574.

- Bucher, K., & Frey, M. (1994). Metamorphism of Granitoids. In *Petrogenesis of Metamorphic Rocks* (pp. 303-308). Springer, Berlin, Heidelberg.


- Bucher, K., & Frey, M. (1994). Metamorphism of Granitoids. In *Petrogenesis of Metamorphic Rocks* (pp. 303-308). Springer, Berlin, Heidelberg.


- Burg, J. P., Guiraud, M., Chen, G. M., & Li, G. C. (1984). Himalayan metamorphism and deformations in the North Himalayan Belt (southern Tibet, China). *Earth and Planetary Science Letters*, *69*(2), 391-400.
- Butt, K. A., & Shah, Z. (1985). Discovery of blue beryl from Ilum granite and its implications on the genesis of emerald mineralization in Swat district. *Geological Bulletin University of Peshawar*, *18*, 75-81.
- Chaudhry, M. N. (1992). *Mail) N* (Doctoral dissertation, University of Peshawar).
- Chauvet, F., Lapierre, H., Bosch, D., Guillot, S., Mascle, G., Vannay, J. C., ... & Keller, F. (2008). Geochemistry of the Panjal Traps basalts (NW Himalaya): records of the Pangea Permian break-up. *Bulletin de la Société géologique de France*, *179*(4), 383-395.
- Coggan, J. S., Stead, D., Howe, J. H., & Faulks, C. I. (2013). Mineralogical controls on the engineering behavior of hydrothermally altered granites under uniaxial compression. *Engineering geology*, *160*, 89-102.
- Colchen, M., Mascle, G., & Van Haver, T. (1986). Some aspects of collision tectonics in the Indus Suture Zone, Ladakh. *Geological Society, London, Special Publications*, *19*(1), 173-184.
- Coleman, M. E. (1996). Orogen-parallel and orogen-perpendicular extension in the central Nepalese Himalayas. *Geological Society of America Bulletin*, *108*(12), 1594-1607.
- Coward, M. P., & Butler, R. W. H. (1985). Thrust tectonics and the deep structure of the Pakistan Himalaya. *Geology*, *13*(6), 417-420.
- Coward, M. P., Butler, R. W. H., Chambers, A. F., Graham, R. H., Izatt, C. N., Khan, M. A., ... & Williams, M. P. (1988). Folding and imbrication of the Indian crust during Himalayan collision. *Philosophical Transactions of the Royal Society of London. Series A, Mathematical and Physical Sciences*, *326*(1589), 89-116.
- Coward, M. P., Jan, M. Q., Rex, D., Tarney, J., Thirlwall, M. T., & Windley, B. F. (1982). Geo-tectonic framework of the Himalaya of N Pakistan. *Journal of the Geological Society*, *139*(3), 299-308.

- D'Andrea, D. V., Fischer, R. L., & Fogelson, D. E. (1965). *Prediction of compressive strength from other rock properties* (Vol. 6702). US Department of the Interior, Bureau of Mines.
- Debon, F., Le Fort, P., Dautel, D., Sonet, J., & Zimmermann, J. L. (1987). Granites of western Karakorum and northern Kohistan (Pakistan): a composite Mid-Cretaceous to upper Cenozoic magmatism. *Lithos*, *20*(1), 19-40.
- DeCelles, P. G., Gehrels, G. E., Quade, J., & Ojha, T. P. (1998). Eocene-early Miocene foreland basin development and the history of Himalayan thrusting, western and central Nepal. *Tectonics*, *17*(5), 741-765.
- Desio, A. (1963). Review of the geologicformations' of the western Karakoram (Central Asia). *Rivista italiana di Paleontologia e Stratigrafia*, *69*(4), 475-501.
- Desio, A. (1964). *Geological Tentative Map of the Western Karakorum 1: 500000*. Institute of Geology.
- Desio, A. (1974). Karakorum mountains. *Geological Society, London, Special Publications*, *4*(1), 255-266.
- Desio, A. (1979). *Geologic evolution of the Karakorum*. Instituti di geologica e paleontologia, Universita degli studi di Milano.
- DiPietro, J. A. (1990). Stratigraphy, structure, and metamorphism near Saidu Sharif, Lower Swat Pakistan.
- DiPietro, J. A., & Pogue, K. R. (2004). Tectonostratigraphic subdivisions of the Himalaya: A view from the west. *Tectonics*, *23*(5).
- DiPietro, J. A., Hussain, A., Ahmad, I., & Khan, M. A. (2000). The Main Mantle Thrust in Pakistan: its character and extent. *Geological Society, London, Special Publications*, *170*(1), 375-393.
- DiPietro, J. A., Pogue, K. R., Hussain, A., & Ahmad, I. (1999). Geologic map of the Indus syntaxis and surrounding area, northwest Himalaya, Pakistan. *Special Papers-Geological Society of America*, 159-178.
- DiPietro, J. A., Pogue, K. R., Lawrence, R. D., Baig, M. S., Hussain, A., & Ahmad, I. (1993). Stratigraphy south of the Main Mantle thrust, lower Swat, Pakistan. *Geological Society, London, Special Publications*, *74*(1), 207-220.
- Dixey, F. (1975). Book Review: A geology for engineers. FGH Blyth and MH de Freitas. Edward Arnold, London. 1974, 557 pp.,£ 7.50 (boards);£ 3.75 (paperback). *Journal of Hydrology*, *26*(1), 176-176.

- Farmer, I. W. (1983). Engineering Description of Rocks. In *Engineering Behaviour of Rocks* (pp. 1-32). Springer, Dordrecht.
- Gaetani, M., & Garzanti, E. (1991). Multicyclic history of the Northern India continental margin (Northwestern Himalaya) (1). *AAPG Bulletin*, *75*(9), 1427-1446.
- Gaetani, M., Angiolini, L., Nicora, A., Sciunnach, D., Le Fort, P., Tanoli, S., & Khan, A. (1996). Reconnaissance geology in upper Chitral, Baroghil and Karambar districts (northern Karakorum, Pakistan). *Geologische Rundschau*, *85*(4), 683-704.
- Gansser, A. (1964). Geology of the Himalayas.
- Gansser, A. (1980). The significance of the Himalayan suture zone. *Tectonophysics*, *62*(1-2), 37-52.
- Gansser, A. (1981). The geodynamic history of the Himalaya. *Zagros Hindu Kush Himalaya Geodynamic Evolution*, *3*, 111-121.
- Garzanti, E., Baud, A., & Mascle, G. (1987). Sedimentary record of the northward flight of India and its collision with Eurasia (Ladakh Himalaya, India). *Geodinamica Acta*, *1*(4-5), 297-312.
- Garzanti, E., Casnedi, R., & Jadoul, F. (1986). Sedimentary evidence of a Cambro-Ordovician orogenic event in the north western Himalaya. *Sedimentary Geology*, *48*(3-4), 237-265.
- Harrison, J. B. (1993). *U.S. Patent No. 5,266,300*. Washington, DC: U.S. Patent and Trademark Office.
- Heim, A., and A. Gansser (1939), Central Himalaya-Geological observations of Swiss expedition, 1936, *Mem. Soc. Helv. Sci. Nat.*, **73**, 1–245.
- Hodges, K. V. (2000). Tectonics of the Himalaya and southern Tibet from two perspectives. *Geological Society of America Bulletin*, *112*(3), 324-350.
- Howarth, D. F., & Rowlands, J. C. (1987). Quantitative assessment of rock texture and correlation with drillability and strength properties. *Rock mechanics and rock engineering*, *20*(1), 57-85.
- Howarth, D. F., & Rowlands, J. C. (1987, August). The effect of rock texture on drillability and mechanical rock properties. In *6th ISRM Congress*. OnePetro.
- Irfan, T. Y. (1996). Mineralogy, fabric properties and classification of weathered granites in Hong Kong. *Quarterly Journal of Engineering Geology and Hydrogeology*, *29*(1), 5-35.

- Irfan, T. Y., & Dearman, W. R. (1978). Engineering classification and index properties of a weathered granite. *Bulletin of the International Association of Engineering Geology-Bulletin de l'Association Internationale de Géologie de l'Ingénieur*, *17*(1), 79-90.
- Jan, M. Q., & Kazmi, A. H. (2005, September). Plate tectonic configuration of gemstones of Pakistan. In *1st Kashmir international conference* (Vol. 20, p. 21).
- Jan, M. Q., & Tahirkheli, R. A. (1969). The geology of the lower part of Indus Kohistan (Swat), West Pakistan. *Journal of Himalayan Earth Sciences*, *4*.
- Jan, M. Q., & Tahirkheli, R. A. (1969). The geology of the lower part of Indus Kohistan (Swat), West Pakistan. *Journal of Himalayan Earth Sciences*, *4*.
- Jan, M. Q., & WINDLEY, B. F. (1990). Chromian spinel-silicate chemistry in ultramafic rocks of the Jijal complex, Northwest Pakistan. *Journal of Petrology*, *31*(3), 667-715.
- Jan, M. Q., Kamal, M., & Khan, M. I. (1981). Tectonic control over emerald mineralization in Swat. *Geol. Bull. Univ. Peshawar*, *14*, 101-9.
- Johnson, R. B., & DeGraff, J. V. (1988). Principles of engineering geology.
- Jumikis, A. R. (1983). Rock mechanics.
- Kazmi, A. H., & Jan, M. Q. (1997). *Geology and tectonics of Pakistan*. Graphic publishers.
- Kazmi, A. H., Lawrence, R. D., Anwar, J., Snee, L. W., & Hussain, S. (1986). Mingora emerald deposits (Pakistan); suture-associated gem mineralization. *Economic Geology*, *81*(8), 2022-2028.
- Khalil, Y. S., Arif, M., Bangash, H. A., Sajid, M., & Muhammad, N. (2015). Petrographic and structural controls on geotechnical feasibility of dam sites: implications from investigation at Sher Dara area (Swabi), north-western Pakistan. *Arabian Journal of Geosciences*, *8*(7), 5067-5079.
- Khan, M. A., Jan, M. Q., & Weaver, B. L. (1993). Evolution of the lower arc crust in Kohistan, N. Pakistan: temporal arc magmatism through early, mature and intra-arc rift stages. *Geological Society, London, Special Publications*, *74*(1), 123-138.
- Khan, M. R., Hameed, F., Mughal, M. S., Basharat, M., & Mustafa, S. (2016). Tectonic study of the Sub-Himalayas based on geophysical data in Azad Jammu and Kashmir and northern Pakistan. *Journal of Earth Science*, *27*(6), 981-988.

- King, B.H. 1964. *The structure and petrology of part of Lower Swat, West Pakistan, with special reference to the origin of the granitic gneisses*. PhD Thesis, University of London.
- Klootwijk, C. T., Gee, J. S., Peirce, J. W., Smith, G. M., & McFadden, P. L. (1992). An early India-Asia contact: paleomagnetic constraints from Ninetyeast ridge, ODP Leg 121. *Geology*, *20*(5), 395-398.
- Larson, K. P., Ali, A., Shrestha, S., Soret, M., Cottle, J. M., & Ahmad, R. (2019). Timing of metamorphism and deformation in the Swat valley, northern Pakistan: Insight into garnet-monazite HREE partitioning. *Geoscience Frontiers*, *10*(3), 849-861.
- Lavé, J., & Avouac, J. P. (2000). Active folding of fluvial terraces across the Siwaliks Hills, Himalayas of central Nepal. *Journal of Geophysical Research: Solid Earth*, *105*(B3), 5735-5770.
- Le Fort, P. (1975). Himalayas: the collided range. Present knowledge of the continental arc. *American Journal of Science*, *275*(1), 1-44.
- Le Fort, P. (1986). Metamorphism and magmatism during the Himalayan collision. *Geological Society, London, Special Publications*, *19*(1), 159-172.
- Le Fort, P. (1996). Evolution of the Himalaya. *The Tectonic Evolutioin of Asia*, *666*.
- Le Fort, P., & Gaetani, M. (1998). Introduction to the geological map of the western Central Karakorum, North Pakistan. Hindu Raj, Ghamubar and Darkot regions. 1: 250,000. *Geologica*, *3*, 3-57.
- Lindqvist, J. E., Åkesson, U., & Malaga, K. (2007). Microstructure and functional properties of rock materials. *Materials characterization*, *58*(11-12), 1183-1188.
- Martin, N. R., Siddiqui, S. F. A., & King, B. H. (1962). A geological reconnaissance of the region between the Lower Swat and Indus rivers of Pakistan. *Geol. Bull. Punjab Univ*, *2*, 1-13.
- McPhie, J. (1993). *Volcanic textures: a guide to the interpretation of textures in volcanic rocks*.
- McPhie, J. (1993). *Volcanic textures: a guide to the interpretation of textures in volcanic rocks*.
- Molnar, P., & Tapponnier, P. (1975). Cenozoic Tectonics of Asia: Effects of a Continental Collision: Features of recent continental tectonics in Asia can be interpreted as results of the India-Eurasia collision. *science*, *189*(4201), 419-426.

- MonaLisa, K. A. (2005). Tectonic model of NW Himalayan fold and thrust belt on the basis of focal mechanism studies. *Pak J Meteorol*, *2*(4), 9-50.
- Morgenstern, N. R., & Eigenbrod, K. D. (1974). Classification of agrillaceous soils and rocks. *Journal of Geotechnical and Geoenvironmental Engineering*, *100*(Proc Paper 10885 Proceeding).
- Mustafa, S., Khan, M. A., Khan, M. R., Sousa, L. M., Hameed, F., Mughal, M. S., & Niaz, A. (2016). Building stone evaluation—A case study of the sub-Himalayas, Muzaffarabad region, Azad Kashmir, Pakistan. *Engineering Geology*, *209*, 56-69.
- Oda, M. (1982). Fabric tensor for discontinuous geological materials. *Soils and foundations*, *22*(4), 96-108.
- Palmer-Rosenberg, P. S. (1985). Himalayan deformation and metamorphism of rocks south of the Main Mantle Thrust, Karakar Pass area, southern Swat, Pakistan.
- Papritz, K. (1989). Evidence for the occurrence of Permian Panjal Trap Basalts in the Lesser and Higher Himalayas of the western syntaxis area, NE Pakistan. *Ecologae Geologicae Helvetiae*, *82*, 603-627.
- PETROGRAPHY, G. *Muhammad Sajid* (Doctoral dissertation, CENTER OF EXCELLENCE IN GEOLOGY, UNIVERSITY OF PESHAWAR).
- Petterson, M. G., & Treloar, P. J. (2004). Volcanostratigraphy of arc volcanic sequences in the Kohistan arc, North Pakistan: volcanism within island arc, back-arc-basin, and intra-continental tectonic settings. *Journal of Volcanology and Geothermal Research*, *130*(1-2), 147-178.
- Petterson, M. G., & Windley, B. F. (1991). Changing source regions of magmas and crustal growth in the Trans-Himalayas: evidence from the Chalt volcanics and Kohistan batholith, Kohistan, northern Pakistan. *Earth and Planetary Science Letters*, *102*(3-4), 326-341.
- Pognante, U., Castelli, D., Benna, P., Genovese, G., Oberli, F., Meier, M., & Tonarini, S. (1990). The crystalline units of the High Himalayas in the Lahul–Zanskar region (northwest India): Metamorphic–tectonic history and geochronology of the collided and imbricated Indian plate. *Geological Magazine*, *127*(2), 101-116.
- Pogue, K. R., DiPietro, J. A., Khan, S. R., Hughes, S. S., Dilles, J. H., & Lawrence, R. D. (1992). Late Paleozoic rifting in northern Pakistan. *Tectonics*, *11*(4), 871-883.

- Pogue, K. R., Hylland, M. D., Yeats, R. S., Khattak, W. U., & Hussain, A. (1999). Stratigraphic and structural framework of Himalayan foothills, northern Pakistan. *SpecialPapers-Geological Society of America*, 257-274.
- Powell, C. M., Roots, S. R., & Veevers, J. J. (1988). Pre-breakup continental extension in East Gondwanaland and the early opening of the eastern Indian Ocean. *Tectonophysics*, *155*(1-4), 261-283.
- Price, D. G. (1995). Weathering and weathering processes. *Quarterly Journal of Engineering Geology and Hydrogeology*, *28*(3), 243-252.
- Price, D. G. (2008). *Engineering geology: principles and practice*. Springer Science & Business Media.
- Pudsey, C. J., Coward, M. P., Luff, I. W., Shackleton, R. M., Windley, B. F., & Jan, M. Q. (1985). Collision zone between the Kohistan arc and the Asian plate in NW Pakistan. *Earth and Environmental Science Transactions of The Royal Society of Edinburgh*, *76*(4), 463-479.
- Räisänen, M. (2004). Relationships between texture and mechanical properties of hybrid rocks from the Jaala–Iitti complex, southeastern Finland. *Engineering geology*, *74*(3-4), 197-211.
- Sajid, M., & Arif, M. (2015). Reliance of physico-mechanical properties on petrographic characteristics: consequences from the study of Utla granites, north-west Pakistan. *Bulletin of Engineering Geology and the Environment*, *74*(4), 1321-1330.
- Sajid, M., Arif, M., & Muhammad, N. (2009). Petrographic characteristics and mechanical properties of rocks from Khagram-Razagram area, Lower Dir, NWFP, Pakistan. *Journal of Himalayan Earth Sciences*, *42*, 25-36.
- Schärer, U., & Allègre, C. J. (1983). The Palung granite (Himalaya); high-resolution UPb systematics in zircon and monazite. *Earth and Planetary Science Letters*, *63*(3), 423 432.
- Searle, M. P. (1991). *Geology and tectonics of the Karakoram Mountains*. John Wiley & Son Incorporated.
- Searle, M. P., & Tirrul, R. (1991). Structural and thermal evolution of the Karakoram crust. *Journal of the Geological Society*, *148*(1), 65-82.
- Searle, M. P., Khan, M. A., Fraser, J. E., Gough, S. J., & Jan, M. Q. (1999). The tectonic evolution of the Kohistan-Karakoram collision belt along the Karakoram Highway transect, north Pakistan. *Tectonics*, *18*(6), 929-949.

- Searle, M. P., Weinberg, R. F., & Dunlap, W. J. (1998). Transpressional tectonics along the Karakoram fault zone, northern Ladakh: constraints on Tibetan extrusion. *Geological Society, London, Special Publications*, *135*(1), 307-326.
- Searle, M., Corfield, R. I., Stephenson, B. E. N., & McCarron, J. O. E. (1997). Structure of the North Indian continental margin in the Ladakh–Zanskar Himalayas: implications for the timing of obduction of the Spontang ophiolite, India–Asia collision and deformation events in the Himalaya. *Geological Magazine*, *134*(3).
- SHAKOOR, A., & BONELLI, R. E. (1991). Relationship between petrographic characteristics, engineering index properties, and mechanical properties of selected sandstones. *Bulletin of the Association of Engineering Geologists*, *28*(1), 55-71.
- SHAKOOR, A., & BONELLI, R. E. (1991). Relationship between petrographic characteristics, engineering index properties, and mechanical properties of selected sandstones. *Bulletin of the Association of Engineering Geologists*, *28*(1), 55-71.
- Shams, F. A. "Geology of the Mansehra-Amb State area Northern West Pakistan." *Geol. Bull. Punjab Univ* 8, no. 1 (1969).
- Sheikh, L., Lutfi, W., Zhao, Z., & Awais, M. (2020). Geochronology, trace elements and Hf isotopic geochemistry of zircons from Swat orthogneisses, Northern Pakistan. *Open Geosciences*, *12*(1), 148-162.
- Sousa, L. M. (2013). The influence of the characteristics of quartz and mineral deterioration on the strength of granitic dimensional stones. *Environmental earth sciences*, *69*(4), 1333-1346.
- Tahirkheli, R. K. (1979). Geology of Kohistan and adjoining Eurasian and Indo-Pakistan continents, Pakistan. *Geol. Bull. Univ. Peshawar*, *11*(1), 1-30..
- Tahirkheli, R. K. (1982). Geology of the Himalaya, Karakoram and Hindukush in Pakistan. *Geological Bulletin, University of Peshawar*, *15*, 1-51.
- Thakur, V. C. (1981). Regional framework and geodynamic evolution of the Indus-Tsangpo suture zone in the Ladakh Himalayas. *Earth and Environmental Science Transactions of The Royal Society of Edinburgh*, *72*(2), 89-97.
- Thakur, V. C., & Misra, D. K. (1984). Tectonic framework of the Indus and Shyok suture zones in eastern Ladakh, northwest Himalaya. *Tectonophysics*, *101*(3-4), 207-220.
- Treloar, P. J., Rex, D. C., Guise, P. G., Coward, M. P., Searle, M. P., Windley, B. F., ... & Luff, I. W. (1989). K-Ar and Ar-Ar geochronology of the Himalayan collision in

NW Pakistan: Constraints on the timing of suturing, deformation, metamorphism and uplift. *Tectonics*, *8*(4), 881-909.

- Tsiambaos, G., & Sabatakakis, N. (2004). Considerations on strength of intact sedimentary rocks. *Engineering Geology*, *72*(3-4), 261-273.
- Tuğrul, A., & Gürpinar, O. (1997). A proposed weathering classification for basalts and their engineering properties (Turkey). *Bulletin of Engineering Geology and the Environment*, *55*(1), 139-149.
- Tugrul, A., & GÜRPINAR, O. (1997). The effect of chemical weathering on the engineering properties of Eocene basalts in northeastern Turkey. *Environmental & Engineering Geoscience*, *3*(2), 225-234.
- Tuğrul, A., & Zarif, I. H. (1999). Correlation of mineralogical and textural characteristics with engineering properties of selected granitic rocks from Turkey. *Engineering geology*, *51*(4), 303-317.
- Ündül, Ö., & Tuğrul, A. (2012). The influence of weathering on the engineering properties of dunites. *Rock Mechanics and Rock Engineering*, *45*(2), 225-239.
- Valdiya, K. S. (1980). *Geology of kumaun lesser Himalaya*. Wadia Institute of Himalayan Geology.
- Weinberg, R. F., & Searle, M. P. (1998). The Pangong Injection Complex, Indian Karakoram: a case of pervasive granite flowthrough hot viscous crust. *Journal of the Geological Society*, *155*(5), 883-891.
- Willard, R. J., & McWilliams, J. R. (1969, January). Microstructural techniques in the study of physical properties of rock. In *International Journal of Rock Mechanics and Mining Sciences & Geomechanics Abstracts* (Vol. 6, No. 1, pp. 1-12). Pergamon.
- Willard, R. J., & McWilliams, J. R. (1969, January). Microstructural techniques in the study of physical properties of rock. In *International Journal of Rock Mechanics and Mining Sciences & Geomechanics Abstracts* (Vol. 6, No. 1, pp. 1-12). Pergamon.
- Willard, R. J., & McWilliams, J. R. (1969, July). Effect of loading rate on transgranular-intergranular fracture in charcoal gray granite. In *International Journal of Rock Mechanics and Mining Sciences & Geomechanics Abstracts* (Vol. 6, No. 4, pp. 415-421). Pergamon.
- Yeats, R. S., & Lillie, R. J. (1991). Contemporary tectonics of the Himalayan frontal fault system: folds, blind thrusts and the 1905 Kangra earthquake. *Journal of Structural Geology*, *13*(2), 215-225.

- Yılmaz, N. G., Goktan, R. M., & Kibici, Y. (2011). An investigation of the petrographic and physico-mechanical properties of true granites influencing diamond tool wear performance, and development of a new wear index. *Wear*, *271*(5-6), 960-969.
- Zanchi, A., & Gaetani, M. (2011). The geology of the Karakoram range, Pakistan: the new 1: 100,000 geological map of Central-Western Karakoram. *Italian journal of Geosciences*, *130*(2), 161-262.
- Zanchi, A., Gaetani, M., & Poli, S. (1997). The Rich Gol Metamorphic Complex: evidence of separation between Hindu Kush and Karakorum (Pakistan). *Comptes Rendus de l'Académie des Sciences-Series IIA-Earth and Planetary Science*, *325*(11), 877-882.

Turnitin Originality Report

Effect of petrographic characteristics on physico-mechanical properties of Granitic gneisses from Islampur and Shir Atraf areas, Swat, NW Pakistan. by Ilyas Mehmood Muhsin .

From CL QAU (DRSML)

- Processed on 24-Feb-2022 09:56 PKT
- ID: 1769694064
- Word Count: 12554

Similarity Index
15%
Similarity by Source

Internet Sources:
10%
Publications:
7%
Student Papers:
5%

**sources:**

1 3% match (Internet from 25-Dec-2016)
https://ore.exeter.ac.uk/repository/bitstream/handle/10871/24651/SajidM.pdf?isAllowed=y&sequence=1

2 2% match (student papers from 26-Jul-2011)
Submitted to Higher Education Commission Pakistan on 2011-07-26

3 2% match (publications)
Tanveer Ahmad. "Mineralogical and textural influence on physico-mechanical properties of selected granitoids from Besham Syntaxis, Northern Pakistan", Acta Geodynamica et Geomaterialia, 2021

4 2% match (Internet from 08-Nov-2014)
http://nceg.upesh.edu.pk/Thesis/MPhil/Thesis61/MuhammadSajidThesis-2012.pdf

5 1% match (publications)
Joseph A. Dipietro, Kevin R. Pogue, Robert D. Lawrence, Mirza S. Baig, Ahmad Hussain, Irshad Ahmad. "Stratigraphy south of the Main Mantle Thrust, Lower Swat, Pakistan", Geological Society, London, Special Publications, 1993

6 < 1% match (student papers from 16-Feb-2018)
Submitted to Higher Education Commission Pakistan on 2018-02-16

7 < 1% match (student papers from 27-Sep-2018)
Submitted to Higher Education Commission Pakistan on 2018-09-27